Atmos. Chem. Phys. Discuss., 13, 19121–19171, 2013
www.atmos-chem-phys-discuss.net/13/19121/2013/
doi:10.5194/acpd-13-19121-2013

Atmospheric Chemistry and Physics Discussions
Open Access

Analysis of the diurnal development of the *Ora del Garda* wind in the Alps from airborne and surface measurements

L. Laiti[1,2], D. Zardi[1,2], M. de Franceschi[1,2,3], and G. Rampanelli[1,2,4]

[1]Atmospheric Physics Group – Department of Civil, Environmental and Mechanical Engineering – University of Trento, Trento, Italy
[2]CINFAI – National Consortium of Universities for Atmospheric and Hydrospheric Physics, Rome, Italy
[3]Diocese of Bolzano-Bressanone, Bressanone, Italy
[4]Depuration Agency – Autonomous Province of Trento, Trento, Italy

Received: 11 March 2013 – Accepted: 14 June 2013 – Published: 18 July 2013

Correspondence to: L. Laiti (lavinia.laiti@unitn.it)

Published by Copernicus Publications on behalf of the European Geosciences Union.

Abstract

A lake-breeze and valley-wind coupled circulation system, known as *Ora del Garda*, typically arises in the late morning from the northern shorelines of Lake Garda (south-eastern Italian Alps), and then channels into the Sarca and Lakes valleys to the north. After flowing over an elevated saddle, in the early afternoon this wind breaks out from the west into the nearby Adige Valley, hindering the regular development of the local up-valley wind by producing a strong and gusty anomalous flow in the area.

Two targeted flights of an equipped motorglider were performed in the morning and afternoon of 23 August 2001 in the above valleys, exploring selected vertical slices of the atmosphere, from the lake's shore to the area where the two local airflows interact. At the same time, surface observations were collected during an intensive field measurement campaign held in the interaction area, as well as from routinely-operated weather stations disseminated along the whole study area, allowing the analysis of the different stages of the *Ora del Garda* development. From airborne measurements, an atmospheric boundary-layer (ABL) vertical structure, typical of deep Alpine valleys, was detected in connection with the wind flow, with rather shallow (~ 500 m) convective mixed layers surmounted by deeper, weakly stable layers. On the other hand, close to the lake's shoreline the ABL was found to be stabilized down to very low heights, as an effect of the onshore advection of cold air by the lake breeze.

Airborne potential temperature observations were mapped over high-resolution 3-D grids for each valley section explored by the flights, using a geostatistical technique called residual kriging (RK). RK-regridded fields revealed fine-scale features and inhomogeneities of ABL thermal structures associated with the complex thermally-driven wind field developing in the valleys. The combined analysis of surface observations and RK-interpolated fields revealed an irregular propagation of the lake-breeze front in the lower part of the valley, and cross-valley thermal asymmetries amenable both to the differential solar heating of the valley slopes and to the valley curvature in its upper part. The overflowing of the potentially cooler *Ora del Garda* air from the Lakes Val-

ACPD
13, 19121–19171, 2013

ley in the afternoon produces a strong katabatic wind at the bottom of the underlying Adige Valley, which blows in cross-valley (i.e. westerly) direction and impinges on the opposite eastern valley sidewall. RK-regridded potential temperature field highlighted that this phenomenon gives origin to a "hydraulic jump" flow structure in the urban area north of the city of Trento, leading to the down-stream formation of a ~ 1300 m deep well-mixed layer.

The improved knowledge of the typical *Ora del Garda* flow patterns and associated ABL structures, deriving from the combined analysis of surface and airborne observations, has practical application in air quality forecasting for the study area, for it helps in the understanding of pollution transport and dispersion processes by thermally-driven winds in the region. Moreover, 3-D meteorological fields produced by RK are likely to be an excellent basis for comparison with results from high-resolution numerical simulations, as they provide a degree of spatial detail that is fully comparable to the spatial scales resolved by large-eddy simulations.

1 Introduction

The differential heating of water/land surfaces and overlying air columns produces thermally-driven local wind systems in coastal regions, known as sea/lake and land breezes. On fair-weather days these daily-periodic circulations blow across the shoreline, regularly reversing their direction between day (onshore) and night (offshore). Sea/lake breezes deeply affect local weather and climate (Simpson 1994), as well as air quality (Lyons and Olsson, 1973; Keen and Lyons, 1978; Drobinski et al., 2007; Boyouk et al., 2011). Accordingly, as a large part of the human population lives in coastal urban areas, breezes developing over seas and large lakes are among the most extensively investigated thermally-driven wind systems, as proved by many theoretical, observational and numerical studies dealing with them (see for example Atkinson, 1981; Pielke, 1984; Simpson, 1994; Crosman and Horel, 2010; Sills et al., 2011). On the contrary, until now only a few research works have focused on breezes arising over small

ACPD
13, 19121–19171, 2013

lakes, i.e. lakes whose characteristic width is less than 50 km, according to the survey of observational studies on small lakes by Segal et al. (1997). Indeed, a comprehensive analysis of such circulations is prevented by the great diversity in size, shape, surrounding topography and land use of small lakes. However, numerical simulations of the airflow developing over idealized circular lakes by Neumann and Mahrer (1975) and Boybeyi and Raman (1992) revealed that smaller lakes produce weaker winds and less well-developed breeze fronts. More recently, Crosman and Horel (2012) carried out a systematic evaluation of the sensitivity of lake-breeze intensity, depth and inland extent to lake size, by gradually varying the lake's diameter in idealized large-eddy simulations. They determined that lake breezes may be considered equivalent to sea breezes for lakes whose characteristic dimension is larger than 100 km, in good accordance with the threshold value of 80 km determined by Segal et al. (1997). They also found that for smaller lakes the dependence of flow features on lake's diameter is low during the late morning but very high in the afternoon.

In the presence of complex coastal orography, sea/lake breezes typically couple with thermotopographically-driven circulations, such as slope, valley and plain-mountain winds (see Zardi and Whiteman, 2013 for a thorough review of these diurnal winds). They are also originated by the differential heating of adjacent air masses, and characterized by a reversal of the flow direction twice per day, similarly to water breezes (Defant, 1951). When these interacting multi-scale circulation systems blow in phase with the sea/lake breeze and no orographic blocking occurs, the resulting flow may display stronger intensities and farther inland penetration than for plain coastal areas, as an effect of the enhancement of the forcing temperature gradients. Indeed, Mahrer and Pielke (1977) showed that up-slope winds developing close to a coastline intensify the local sea breeze. Kondo's (1990b) idealized numerical simulations of sea-breeze variability in connection with different topographic configurations revealed a pronounced strengthening associated with the presence of a valley mouth in front of the coast, and the development of a regional-scale unified flow, the so-called Extended Sea Breeze. A multi-scale unified wind system, referred to as Extended Lake Breeze, was identified on the basis of detailed observations and numerical results also for the Alpine basin of the small Lake Tekapo, New Zealand (McGowan et al., 1995; McGowan and Sturman, 1996; Kossmann et al., 2002). Bastin et al. (2005) reported the different effect of two large valleys facing the Mediterranean Sea near Marseille (France), i.e. the Rhône Valley and the Durance Valley, on the local sea breeze: while the former does not display any significant influence, the presence of the narrower Durance Valley increases the wind speed by channelling the flow. Moreover, numerical simulations by Bergström and Juuso (2006) provided evidence of the fact that a continuous source of cold air (i.e. a lake) at a valley bottom produces stronger up-valley winds, for it magnifies and maintains the thermal contrast forcing the up-valley wind onset. It follows that "extended" wind systems produced by the coupling of mountain winds and water breezes are able to transport airborne pollutants on longer distances than "pure" coastal or valley circulations, severely affecting air quality in areas far from emission sites and giving origin to elevated pollution layers, as discussed for example by Carroll and Baskett (1979), Kitada et al. (1986), Wakimoto and McElroy (1986), Kondo (1990a,b), Lu and Turco (1994, 1995) and Pérez-Landa et al. (2007).

The present paper focuses on a peculiar case of interaction between the lake breeze induced by a small lake (maximum width: 16 km) lying at the inlet of a deep Alpine valley and the local up-valley flow. This coupled wind, which is known as *Ora del Garda*, arises over the northern shorelines of Lake Garda in the southeastern Italian Alps, and then channels northward into the Sarca and Lakes valleys, until overflowing into the adjacent Adige Valley through an elevated pass. Here it hinders the regular development of the local up-valley wind, producing an anomalous cross-valley flow characterized by strong gusts. Various authors contributed in the past to the investigation of the *Ora del Garda* wind (Defant, 1909; Schaller, 1936; Pollak, 1924; Wiener, 1929; Wagner, 1938; Daves et al., 1998; Baldi et al., 1999; Zardi et al., 1999). More recently, during summer 2001, the Atmospheric Physics Group of the University of Trento carried out a targeted measurement campaign, including both intensive surface observations (de Franceschi et al., 2002) and two flights of an instrumented motorglider (de Franceschi et al., 2003) that were performed on a well-developed *Ora del Garda* day.

Indeed, the present work aims at the analysis of nature and evolution of the diurnal atmospheric boundary-layer (ABL) structures typically associated with the *Ora del Garda* development, based on the above-cited database and on surface observations from routinely-operated local weather stations. Special focus is given to the interaction area at the junction between the Lakes and the Adige valleys north of Trento city, where intensive surface observations were collected. In particular, airborne measurements allow the retrieval of the fine-scale 3-D variability of the upper atmosphere arising from the heterogeneous spatial distribution of surface sensible heat fluxes, due to underlying complex topography and land cover discontinuities (Rotach and Zardi, 2007). As a matter of fact, instrumented light aircrafts represent very suitable platforms for the investigation of ABL processes over complex terrain, for they can provide high temporal and spatial resolution observations thanks to their good manoeuvrability and flexibility. Equipped light aircrafts were flown for example during the field measurements of the DISKUS experiment (Hennemuth, 1985, 1986; Hennemuth and Schmidt, 1985), the MAP-Riviera project (Weigel and Rotach, 2004; Rotach and Zardi, 2007), the ALPNAP project (Gohm et al., 2009; Harnisch et al., 2009; Schnitzhofer et al., 2009), the ESCOMPTE experiment (Hasel et al., 2005; Puygrenier et al., 2005) and the COPS project (Kalthoff et al., 2009). Similarly, Kraus et al. (1990), Finkele et al. (1995), Stephan et al. (1999) and Wood et al. (1999) used light aircrafts to observe the fine-scale structure of sea-breeze circulation cells. However, in order to visualize fine-scale 3-D structures of the sampled meteorological fields, airborne data collected along flight trajectories need to be appropriately remapped over the explored atmospheric volume. Various simple interpolation techniques may be used, such as inverse distance weighting method (Egger, 1983; Hennemuth, 1985), or natural neighbour method (De Wekker, 2002; Weigel and Rotach, 2004). Laiti et al. (2013a) have recently proposed the application of geostatistical technique called residual kriging (RK) for mapping airborne observations over high-resolution regular grids. In Laiti et al. (2013a,b) RK-gridding of

ACPD
13, 19121–19171, 2013

airborne data has proved useful for the retrieval of 3-D local features of the ABL potential temperature field that would not have been revealed by simple vertical profiles. Accordingly, it is adopted also in the present study.

The paper is organized as follows. Section 2 provides a brief description of the investigated circulation and of the area where it develops. The two measurement flights and the set of surface observations forming the experimental database analysed in this work are then presented in Sect. 3. Section 4 illustrates the methods used for the post-processing of airborne observations in order to remap them over 3-D high-resolution grids through RK application. Section 5 consists in the detailed discussion of diurnal cycles recorded at the surface weather stations disseminated in the study area, as well as of dominant vertical structures and fine-scale 3-D variability of the ABL displayed by interpolated airborne data. Finally, Sect. 6 summarizes the main findings and conclusions, providing an outlook on possible future developments.

2 The Ora del Garda wind

The present paper investigates a lake-breeze and valley-wind coupled circulation, the *Ora del Garda* wind (first scientifically documented by Defant, 1909), which blows on fair-weather, warm-season days over the northern shoreline of Lake Garda, in the southeastern Italian Alps (see Fig. 1 for localization and topography of the target area). The northern branch of Lake Garda is confined on both sides by high mountain ranges (~ 2000 m m.s.l.), resembling a fjord configuration, and it is open only to the north onto the lower Sarca Valley, which consists of a rather wide (~ 5 km) and flat (valley-floor height range: 65–100 m m.s.l.) basin. In the late morning a lake-breeze front propagates inland across this flat area, then the breeze channels up-valley into the nearby Lakes Valley, coupling with the local up-valley winds. A number of small lakes lie in this area: Cavedine and Toblino-S.Massenza lakes are the largest ones (~ 1 km^2 surface). North of Toblino-S.Massenza Lake the valley axis changes its orientation from SSW–NNE to WSW–ENE, and the cross section widens out to the area of the Terlago basin.

ACPD
13, 19121–19171, 2013

An elevated pass, the saddle of Terlago, joins the northernmost end of the Lakes Valley with the underlying Adige Valley, on the western side of the latter. When the thermal forcing is strong enough, the *Ora del Garda* wind breaks out into the Adige Valley from this elevated ridge (see Fig. 1b) in the early afternoon, producing a strong and gusty westerly flow in the area. Hence the local up-valley wind is blocked and forced to flow over a denser wedge of potentially colder air forming above the Adige Valley floor; this cold air mass channels in both northward and southward direction, inducing an anomalous down-valley wind regime up to some kilometres south of the city of Trento (Pollak, 1924; Wiener, 1929; Schaller, 1936; Wagner, 1938; de Franceschi et al., 2002). The inflow from the Lakes Valley persists in the area, although gradually weakening, for a few hours after sunset, then it suddenly ceases and a rather intense down-valley drainage current develops in the Lakes Valley (de Franceschi et al., 2002).

Climatological characterizations of the typical diurnal cycle of the *Ora del Garda* wind, based on observations collected from surface weather stations deployed along the valley floor, have been provided in the preliminary works by Baldi et al. (1999) and Daves et al. (1998), and, more recently, by Giovannini (2012). According to these studies, the *Ora del Garda* typical onset and offset times are 11:00 LST (UTC+1) and 19:00 LST (at Lake Garda's shoreline), while its typical direction and intensity are SSW and 6–7 $\mathrm{m\,s^{-1}}$ respectively. The first outbreak of the wind into the Adige Valley occurs at 14:00 LST; from then onwards, an anomalous and intense westerly (i.e. cross-valley) wind blows at the valley floor, dropping at 21:00 LST. While the characteristic diurnal cycle of the *Ora del Garda* at the surface is rather well understood, little is known about the structure of the upper valley atmosphere associated with the development of this circulation. A first contribution, also based on both airborne and surface observations, is found in Laiti et al. (2013a,b), who detected ABL thermal structures attributable to the development of a lake-breeze front at the shoreline or to asymmetric cross-valley circulations, as well as different up-valley flow depths and stratification conditions for different synoptic situations.

ACPD
13, 19121–19171, 2013

3 The experimental dataset

3.1 Measurement flights

On 23 August 2001 two flights of an instrumented motorglider were performed over the target area. The first flight was carried out in the late morning, and explored the area from Lake Garda's shoreline through the Adige Valley, while the second, held in the early afternoon, overflew only the area north of Trento and the Terlago saddle area. Instruments recorded position, air pressure, temperature and relative humidity with 1 Hz sampling frequency (see de Franceschi et al., 2003 for further technical details about the measurement platform). The motorglider flew a total of eight spiralling trajectories, oriented along specific vertical sections of the valley atmosphere, exploring five different sites:

- site A: the flat-bottomed basin facing Lake Garda, i.e. the lower Sarca Valley;
- site B: the narrow valley stretch joining the lower Sarca Valley with the southern Lakes Valley;
- site C: the central Lakes Valley, at halfway between Cavedine Lake (to the south) and Toblino-S.Massenza Lake (to the north);
- site D: the ending part of the Lakes Valley (i.e. the Terlago basin), close to the ridge of the saddle of Terlago;
- site E: the Adige Valley in front of the saddle of Terlago.

The morning flight (flight #1) covered four sections along the valleys where the *Ora del Garda* wind blows (A, B, C and D sites) and explored twice the E site, while the afternoon flight (flight #2) focused on the area where the interaction between the *Ora del Garda* wind and the Adige Valley wind occurs (D and E sites). The trajectories followed by the two flights are displayed in Fig. 2, and the characteristics of each single spiral

ACPD
13, 19121–19171, 2013

that was flown are reported in Table 1. Unfortunately, GPS data are lacking for the last two spirals of flight #1 (D1 and E1b). Therefore only vertical profiles of the measured variables are available for them. Moreover, both along-valley and cross-valley oriented flight legs were performed over site A, allowing an extensive exploration of the local atmosphere 3-D structure.

3.2 Surface observations

In addition to the research flights, surface observations were collected from automated weather stations (AWSs) belonging to observational networks and routinely operated by local institutions, and mainly deployed along the floor of the target area's valleys. A list of the AWSs considered in the present study and of their technical specifications is given in Table 2. Notice that wind, pressure and radiation data are recorded at some stations only, and that the temporal resolution of the observations is different among networks (15 min vs. 1 h). Beside these routine observations, an intensive field campaign was held between 13 and 24 August 2001 in the area north of Trento where the two local airflows interact. During this campaign two additional weather stations were operated. One was installed at Monte Terlago (720 m m.s.l.; close to the ridge of the Terlago saddle and the NNW valley sidewall, where the maximum wind speed is expected), and recorded 10 min averaged values of 3 m a.g.l. wind speed and direction, air pressure, relative humidity, global and net radiation. The second station consisted in an ultrasonic anemometer installed near a pre-existing AWS at Roncafort, on the Adige Valley floor (195 m m.s.l.), at the foot of the vertical cliff of the Terlago saddle, to evaluate the turbulent fluxes developing in the surface layer in this area (de Franceschi and Zardi, 2003; de Franceschi et al., 2002, 2009; de Franceschi, 2004). The locations of all surface observation sites are indicated in Fig. 2.

ACPD
13, 19121–19171, 2013

3.3 Weather conditions

On 23 August 2001 clear-sky and weak-wind conditions were observed throughout all the day at the crest-level AWSs named PAG and GAZ (respectively 2125 and 1601 m m.s.l.; see Fig. 2). The complete absence of cloud cover in the morning is also shown by satellite images, while in the afternoon some cumulus clouds developed over the target area at mountain-top level, as a result of convergence of thermally-driven circulations. Reanalyses show a high-pressure ridge elongating over central Europe from SW, consistently with the presence of a weak northerly synoptic wind blowing across the Alps, as indicated by routine radiosoundings. Hence, it can be argued that on the flight day good conditions for the full development of thermally-driven circulations occurred, as confirmed by time series of surface observations (see Sect. 5.1).

4 Methods

Time series of surface observations of wind, temperature and humidity at the valley floor allowed the identification of the different stages of the *Ora del Garda* wind development. In addition, ultrasonic anemometer measurements collected at Roncafort site were analysed by means of eddy correlation techniques to obtain values of vertical sensible heat flux at the surface, adopting an averaging period of 30 min (de Franceschi et al., 2002; de Franceschi, 2004). The post-processing techniques applied to the airborne data are described in the following paragraphs.

4.1 Extraction of pseudo-soundings from airborne data

Concerning the analysis of airborne data, since each single valley section explored by the instrumented motorglider was flown in less than 30 min (with the only exception of A1 spiral; see Table 1), the temporal variability over the single section can be neglected, as no appreciable evolution of the ABL structure took place during the overflight time (cf. Stull, 1988). Accordingly, following the procedure described in Laiti et al. (2013a), for each single spiral the dominant vertical structure of the ABL was extracted from airborne observations of potential temperature and mixing ratio, by means of a moving-window vertical average algorithm (window width: 200–250 m). This allowed filtering out high-frequency oscillations associated both with the intrinsic 3-D variability of the sampled meteorological fields (i.e. locally higher potential temperature values associated with convective thermals, or with the up-slope flow layer along the lateral valley sidewalls, etc.) and with the flight pattern itself. These “mean” vertical profiles will be from here onwards referred to as “pseudo-soundings”.

4.2 Residual kriging mapping of airborne data

Following the approach proposed by Laiti et al. (2013a) and adopted in Laiti et al. (2013b), a residual kriging (RK) interpolation technique (also known as “regression kriging” or “detrended kriging”; Ahmed and de Marsily, 1987; Odeh et al., 1994, 1995; Goovaerts, 1999) was applied to map potential temperature airborne data over high-resolution 3-D regular grids (grid spacing: 50 m × 50 m × 50 m), including also surface observations from the AWSs nearest to each single spiralling trajectory (where present). This method reflects the nature of the thermal field of the valley atmosphere, which results from the superimposition of a local anomaly field on an essentially vertical prevailing structure. Indeed, RK foresees the explicit decomposition of the target field $Z(\boldsymbol{x})$ (in our case, the potential temperature field) into a drift component $\mu(\boldsymbol{x})$ and a residual component $\delta(\boldsymbol{x})$:

$$Z(\boldsymbol{x}) = \mu(\boldsymbol{x}) + \delta(\boldsymbol{x}), \tag{1}$$

to be estimated separately at each grid node $\boldsymbol{x}_\alpha$, as follows:

$$\hat{Z}(\boldsymbol{x}_\alpha) = \hat{\mu}(\boldsymbol{x}_\alpha) + \hat{\delta}(\boldsymbol{x}_\alpha) \tag{2}$$

(where the circumflex accent indicates the estimated values of the different components). In particular, the aforementioned pseudo-soundings are here adopted as vertical drift term, while the residuals are interpolated by means of a standard ordinary

ACPD
13, 19121–19171, 2013

kriging algorithm (Cressie, 1993; Goovaerts, 1997). An isotropization of the residual field is preliminarily operated, by rescaling the spatial coordinates according to the characteristic scales of correlation along the horizontal and the vertical direction (typical values: 1000–2000 and 350–550 m respectively). The appropriate scaling factors are inherently provided by directional semivariograms of the residuals. The semivariogram function (whose shape is empirically estimated from the dataset as lag-averaged dissimilarity function between pairs of observations) models the spatial structure of the covariance function specific to the observations, and is fundamental in kriging methods implementation (Cressie, 1993; Goovaerts, 1997). See Laiti et al. (2013a) for further details about the implementation of the RK-mapping procedure.

5 Discussion of results

5.1 *Ora del Garda* diurnal cycle at the surface

As anticipated in Sect. 4, the different stages of the *Ora del Garda* wind were identified for 23 August 2001 on the basis of time series of surface measurements. Selected temperature, wind, radiation and humidity observations collected at the AWSs indicated in Fig. 2 and listed in Table 2 are reported in Figs. 3, 4 and 5. The AWSs are grouped according to their geographic area: (a) the lower Sarca Valley, (b) the Lakes Valley, the Adige Valley both (c) south of Trento and (d) north of Trento. The discussion of the phenomena viewed from data recorded by the stations will follow the same subdivision.

5.1.1 Lower Sarca Valley

Observations collected at RDG (Fig. 3) depict the wind pattern at Lake Garda's shoreline on the flight day: following a pressure maximum and a wind speed minimum, the wind direction abruptly shifts from northerly to southerly at 10:00 LST indicating the onset of the lake breeze, i.e. the formation of a lake-breeze front, which is accompanied by a sudden temperature decrease (Fig. 4a) and increase in water vapour mixing ratio (not shown) (as shown for example in Zumpfe and Horel, 2007). The lake breeze reinforces from 13:00 LST to the maximum intensity of 6.0 $\mathrm{m\,s^{-1}}$ (gust speed: 8.8 $\mathrm{m\,s^{-1}}$) recorded at 14:00 LST, persisting until the local sunset time (18:00 LST) and then rapidly ceasing. Lake Garda's water temperature (measured at RDG) keeps almost constant throughout all the day (~ 21 °C), showing rather low values with respect to daytime air temperature (which contributes to the development of a strong circulation): the average difference is around 7 °C at the breeze onset, and reduces to 5 °C when the wind strengthens in the afternoon. Actually air temperature also shows a very limited range of variation between night and day (only 6.5 °C): in the afternoon RDG temperature curve appears completely flattened around ~ 26.5 °C value. At 11:00 LST a sharp drop in the higher-resolution temperature series collected at TOR and ARC (respectively ~ 1.5 km and ~ 5 km inland from the lake's shoreline) clearly indicates the passage of the lake-breeze cold front at both locations at the same time, despite their different distance from the shoreline. At 11:00 LST a similar signal is recorded also at NAG and TEN (not shown; see Fig. 2 for AWSs' position). This indicates a delayed inland propagation of the front in the easternmost part of the lower Sarca Valley, between Mt. Brione and the eastern sidewalls. At DRO, which lies in the narrow corridor joining the lower Sarca Valley with the Lakes Valley, the morning heating phase ceases from 10:00 LST, then the temperature curve is levelled out (to values ranging between 28 and 30 °C) until 17:00 LST (Fig. 4a). Notice that TOR, ARC and DRO record temperature higher than stations further down-stream (i.e. up-valley; see next section) because they are situated very close to the lateral valley sidewalls, experiencing locally warmer conditions. However, at all the stations of this group the observed temperature cycle is remarkably different from a "standard" diurnal cycle of a fair-weather day, which is normally characterized by a relatively fast morning warming phase, a peak occurring about 2 h after the solar radiation peak, and a slower afternoon decay. Here the temperature pattern during the central hours of the day appears to be completely dominated by the effects of the up-valley advection of cold air from above Lake Garda's surface.

ACPD
13, 19121–19171, 2013

5.1.2 Lakes Valley

CAV and MAS stations lie on the shoreline of Cavedine and Toblino-S.Massenza Lakes respectively, while PIE is located less than 1 km north of Cavedine Lake, i.e. immediately down-stream of this small lake with respect to the *Ora del Garda* flow. In this area the valley floor displays a negligible slope, while north of Toblino-S.Massenza Lake it rapidly rises up to about 600 m m.s.l. (at the Terlago saddle ridge). At the same time, here the valley axis turns from SSW–NNE to WSW–ENE. TER and Monte Terlago stations are both situated in this upper part of the Lakes Valley.

On 23 August 2001 PIE and TER record an increasing wind intensity from 10:00 and 11:00 LST respectively, peaking at 14:00 and 16:00 LST (not shown; maximum wind speed is 3.9 m s^{-1} at TER; corresponding gust speed: 8.7 m s^{-1}). At TER the wind drops around 22:00 LST (not shown). Intensive observations at Monte Terlago (located at short distance from TER, very close to the SE-exposed valley sidewall) show a gradual transition from up-slope to up-valley wind in the morning, completed at 11:50 LST; the up-valley wind strengthens up to ~ 5.5 m s^{-1} between 15:30 and 20:00 LST and then weakens, definitely dropping at 21:50 LST (Fig. 3). Although no clue of a well-defined lake-breeze front passage is given by these AWSs, at all of them the evident flattening of the temperature curve (Fig. 4b) during the diurnal up-valley wind phase reveals the effect of a large source of cold air at the valley bottom, i.e. Lake Garda; indeed, homogenous values around 27–28 °C are recorded, even at the end of the valley at TER (428 m m.s.l.).

5.1.3 Adige Valley – south of Trento

This group of stations is representative of pure up-valley wind conditions in the Adige Valley, free from any interference by the *Ora del Garda* wind (except TNS). On the flight day a southerly up-valley wind blows at ROV from 14:00 to 19:00 LST, with an average speed of 2.6 m s^{-1}; the wind intensity peak is generally recorded around 16:00 LST (e.g. 3.9 m s^{-1} at VOL; not shown). At TNS (~ 5 km south to Trento) the wind blows from S between 13:00 to 18:00 LST (average intensity: 2.0 m s^{-1}), replaced by a weak (0.7 m s^{-1}) northerly flow between 19:00 and 20:00 LST (Fig. 3): this is very likely the effect of the anomalous southward channelling of the *Ora del Garda* airflow along the Adige Valley. At all stations quasi-identical and rather typical diurnal temperature cycles are observed: the temperature increases up to about 32 °C peak value (registered around 15:00 LST), then it gradually decreases during the late afternoon and evening phase (Fig. 4c).

5.1.4 Adige Valley – north of Trento

Stations belonging to this group are located up to 8 km north of the area where the *Ora del Garda* first overflows from the Lakes Valley into the Adige Valley, and most directly affects the local airflow. Weak (1.5 m s^{-1}) up-valley wind conditions are detected around local noon at GAR and RON (Fig. 3), the two stations closest to the Terlago saddle. Associated with the *Ora del Garda* outbreak, a westerly wind is recorded from 14:00 LST at GAR, which lies in the middle of the valley floor, exactly in front of the lowest point (580 m m.s.l.) of the saddle ridge. Only later, at 15:30 LST, a west-northwesterly wind is detected at RON, which is situated in a more sheltered position (1.5 km south to GAR and close to the foot of the quasi-vertical cliff, where the saddle crest-height touches 780 m m.s.l., i.e. 600 m above the valley floor), after a short (∼30 min) northerly flow phase. Indeed, RON high-resolution observations are consistent with the picture of a gradual southward propagation of the denser airmass advected by the *Ora del Garda* (Schaller, 1936) from the point of the main-stream overflow, i.e. the lowest point of the saddle ridge. Then the wind speed increases gradually up to 5 m s^{-1} at both stations; this flow regime suddenly stops first at RON (20:15 LST) and then at GAR (21:00 LST), the maximum wind intensity values being recorded between 16:00 and 18:00 LST at GAR, RON and ZAM, with gusts up to 11.3 m s^{-1} at GAR (not shown).

The associated temperature daily cycle (Fig. 4d) presents specific features, different from those displayed by the "reference" Adige Valley AWSs (see Sect. 5.1.3 and

Fig. 4c): during the central afternoon hours (15:00–18:00 LST) their temperature results lower; in particular, at GAR the air begins to cool down at a quasi-constant rate from 14:00 LST. On the contrary, from 18:00 LST onwards, at all the group stations the temperature is higher than at the "reference" Adige Valley AWSs, and a near constant temperature value ($\sim 27\,^{\circ}$C) is registered until 20:00 LST; then the air cools down, although keeping still warmer than south to Trento until the late evening. This behaviour is to be ascribed to the persistence of the inflow of air from the Lakes Valley in the evening: in the afternoon the air advected by the *Ora del Garda* is potentially cooler than the local air, while in the early evening phase it results warmer; this slows down the cooling of the lowest Adige Valley atmosphere due to the local radiation drop. Accordingly, the diurnal cycle of sensible heat fluxes at the Adige Valley floor (provided by eddy correlation analysis of the ultrasonic anemometer data at Roncafort) shows rather large negative values (in the order of $-100\,\mathrm{W\,m^{-2}}$) starting from the local sunset time, i.e.17:30 LST, until 20:00 LST (see Fig. 5), in connection with the climax of the strong ventilation and turbulence still produced by the *Ora del Garda* in the area.

5.2 Dominant vertical structure of the ABL

This section discusses the vertical structure of the ABL associated with the *Ora del Garda* development, as revealed from pseudo-soundings of potential temperature and mixing ratio extracted from the airborne dataset. In Figs. 6 and 7 they are compared to routine soundings from Milan (LIML) and Udine (LIPD) stations in the Po Valley. In particular pseudo-soundings from flight #1 (09:15–12:15 LST) are compared to 06:00 and 12:00 UTC (i.e., 07:00 and 13:00 LST) sounding, while those from flight #2 (14:15–15:30 LST) with 12:00 and 18:00 UTC (i.e., 13:00 and 19:00 LST) sounding. Surface measurements from the AWSs closest to the area explored by the single spiralling trajectory are also reported in the figure, as representative of the surface layer conditions.

Both in the morning and in the afternoon the typical diurnal heating excess between mountain valley air masses and air masses over the plain (i.e. the Po Valley) is observed: the upper valley atmosphere is on average ~ 1 K potentially warmer throughout the whole explored depth (up to ~ 1 km above the height of the lateral crests). Only A1 and E1 pseudo-soundings are colder than LIML 06:00 and 12:00 UTC sounding (below ~ 1000 m m.s.l.), for in the early morning hours the atmosphere in the Adige Valley and above Lake Garda's surface is still very stably stratified.

5.2.1 Lower Sarca Valley and Lakes Valley

Flight #1, which explored four different sites in the valleys where the *Ora del Garda* flows, was performed during the very initial stages of the breeze development, before its outbreak into the Adige Valley.

A1 pseudo-sounding is representative of the flat basin facing the lake's northern shoreline; at the upper levels it is rather consistent with 06:00 and 12:00 UTC LIML soundings; it is also colder than the following pseudo-soundings at all levels; an elevated quasi-mixed layer (QML), driven by the return flows associated with up-slope circulations (see Kuwagata and Kimura, 1995, 1997), extends between 1500 and 1800 m m.s.l.; below that height the stratification is stable (3 K km^{-1} lapse rate) almost down to the minimum flying height (~ 250 m m.s.l., i.e., ~ 185 m above the lake's surface) (Fig. 6a). Further up-valley B1 and C1 pseudo-soundings in the Lakes Valley look very similar: they show a warmer atmosphere than A1, especially below ~ 1500 m m.s.l. where the lapse rate is reduced to 2 K km^{-1}, due to the subsidence that is locally induced by cross-valley compensation circulation (Kuwagata and Kimura, 1995, 1997; Rampanelli et al., 2004; Serafin and Zardi, 2010a,b, 2011). At both locations a less than 500 m deep ML is detected, slightly colder at B1 than at C1 (ML mean potential temperature θ_m: 300.4 K and 300.7 K respectively; see Table 3). At the end of the Lakes Valley, D1 pseudo-sounding is on average ~ 1 K warmer than B1 and C1 above 1150 m m.s.l. height, and shows two distinct elevated QMLs around 1500 and 2000 m m.s.l.; the 750 m deep ML has a θ_m value of 301.8 K. More than three hours later (D2 pseudo-sounding in Fig. 6b), the ML depth is reduced to 600 m, θ_m has increased by ~ 2 K, and the lapse rate in the layer below 1750 m m.s.l. has been consistently modified by the heating process associated to local subsidence (from 3.5

to 2.0 K km^{-1}). Differently from pseudo-soundings further up-stream (i.e. down-valley), both D1 and D2 display a weak inversion layer at the top of the ML.

To summarize, close to Lake Garda the valley atmosphere is stable down to very low heights or even to the ground, while moving further up-valley (i.e. down-stream) a gradual transition to a rather typical valley ABL pattern occurs: shallow MLs (displaying depths in the order of 500 m) with weak or even absent capping inversion layers are detected, surmounted by deep, weakly stable layers and/or elevated QMLs extending up to the lateral crest height. Such a structure is likely to be originated by the subsidence of the core of the upper valley atmosphere, driven by downward motions compensating for up-slope circulations. This mechanism warms up and stabilizes the upper part of the potential temperature profile during the daytime phase, and also inhibits the convective growth of the surface ML (Kuwagata and Kimura, 1995, 1997; De Wekker et al., 2004; Rampanelli et al., 2004; Rotach and Zardi, 2007; Serafin and Zardi, 2010a,b, 2011). Mixing ratio pseudo-soundings (Fig. 7) confirm this ABL pattern: unlike in standard CBL schemes, the water vapour appears rather uniformly distributed well above the top of the MLs detected at the valley floor, i.e. over the whole valley atmosphere volume up to the average height of the lateral crests (∼ 1500 m m.s.l.). This is very likely associated with the vertical transport and possible redistribution of humidity operated by up-slope winds, exporting water vapour from the valley floor along the lateral sidewalls of the valley (Kuwagata and Kimura, 1995, 1997; Weigel et al., 2007).

5.2.2 Interaction area

Three pseudo-soundings are available for the Adige Valley cross section in front of the Terlago saddle, allowing an evaluation of the evolution of the vertical structure of the valley ABL in the area. From GAR surface observations in Fig. 3 it can be argued that each one of them is representative of a different wind regime: a well-developed down-valley wind (E1a), the transition between down-valley and up-valley wind (E1b), the westerly wind regime following the first *Ora del Garda* outbreak into the Adige Valley

ACPD
13, 19121–19171, 2013

(E2). Between the first two stages (E1a and E1b; Fig. 6b), the cold air mass accumulated on the valley floor during night-time is eroded: the heating results particularly intense in the layer extending from the ground surface up to ~ 1200 m m.s.l., while the atmosphere above maintains the same lapse rate (~ 4 K km^{-1}) and its potential temperature grows only by about 1 K. At the same time, θ_m increases from 296.2 K to 300.6 K, and the ML depth increases from 200 m to 400 m. On the other hand, between noon (E1b) and afternoon (E2) a 2–3 K heating takes place throughout the whole depth of the explored valley atmosphere, the ML depth increases to 1200 m, and θ_m further grows by 3.5 K. Within a slightly longer time interval, over the saddle of Terlago (D site) a significantly smaller heating occurs, especially above 1750 m m.s.l. height, and θ_m increases by only ~ 1.8 K; this suppression of the temperature rise in the valley atmosphere is amenable to the presence of a large, continuous source of cold air at the valley inlet, i.e. Lake Garda, and to the up-valley advection associated with the *Ora del Garda* flow.

Morning pseudo-soundings at D1 (local valley floor: ~500 m m.s.l.) and E1b (local valley floor: ~200 m m.s.l.) are very similar in their upper part, while below 1150 m m.s.l. D1 is ~ 1 K warmer than E1b (θ_m: 301.8 vs. 300.6 K). On the contrary, in the afternoon E2 pseudo-sounding is ~ 1.5 K potentially warmer than D2 above 1600 m m.s.l., while the two profiles display almost equal values below that height, with θ_m slightly lower at D2. The similar mixing ratio values of D2 and E2 also suggest that this is the depth of the layer where the strong mixing between the *Ora del Garda* and the Adige Valley air occurs during the afternoon phases, while air masses with different characteristics are present in the layers above (Fig. 7b). A marked difference between morning and afternoon conditions is also highlighted by surface data collected at the closest AWSs: while in the morning all the observations display values on average ~ 1 K higher than the θ_m value of the corresponding airborne pseudo-sounding, in the afternoon the surface measurements at D and E sites are almost equal to, or even lower than, the associated θ_m. This fact suggests that the intense ventilation produced in the afternoon by the *Ora del Garda* has cooled down the ground in the area, and surface sensible heat fluxes are no longer feeding the ML convective growth in this phase (cf. Sect. 5.1.4). Indeed, as this transition from an unstably-stratified surface layer (which is consistent with the typical daytime CBL structure) to stably-stratified conditions immediately above ground occurs before the local sunset time (i.e. around 18:00 LST at the Adige Valley floor), it cannot be produced by the radiative cooling of the ground surface.

5.3 Fine-scale 3-D structure of the ABL

RK-gridded potential temperature fields allow the identification of fine-scale 3-D features of the thermal structures of the valley ABL at the explored sites, which are discussed in the present section. Notice that the RK-estimated standard deviation of the interpolated (residual) values (i.e. the square root of the RK-estimated variance of the RK-predicted residual values; Cressie, 1993; Goovaerts, 1997) varies in the range 0.00–0.25 K for all the interpolated fields displayed below.

5.3.1 Lower Sarca Valley – Spiral A1

The high-resolution 3-D potential temperature field from spiral A1 (Figs. 8 and 9) reveals a non-uniform propagation of the lake-breeze front from the Lake Garda's shoreline across the lower Sarca Valley: at the time of the site's overflight (~10:00–10:45 LST) colder air is present at the lowest layers in the western half of the valley cross section, compared to the area of Mt. Brione (Fig. 8). Surface observations at TOR and ARC substantiate the hypothesis of an earlier penetration of the lake breeze in the eastern half of the valley: at both AWSs the front passage is detected at 11:00 LST, although the first lies at only 1.5 km from the coastline, between Mt. Brione relief and the eastern valley sidewall, while the second is situated 5 km inland, at the northern side of the basin (see Sect. 5.1.1). A possible explanation for this behaviour is provided by the ~ 1.5 h delay between local sunrise times at the two lateral extremities of the valley bottom (06:05 and 07:45 LST respectively for the western and the eastern extremity, as determined by means of a GIS analysis, which was performed to evaluate

ACPD
13, 19121–19171, 2013

the diurnal cycle of the incoming solar radiation in the area). Topographic shadowing delays the establishment of the water-land temperature contrast that produces the lake breeze. As a consequence, the onset of the latter is retarded in the area close to the eastern valley sidewalls. Moreover, the narrow corridor between Mt. Brione relief and the eastern slopes (width: ~ 500 m) is known to receive a strong drainage flow of cold air during the night until the morning, as this is the last portion of the basin to be sunlit in the morning. This fact could further delay the penetration of the *Ora del Garda* front in the area.

On the other hand, in the upper atmosphere (above 1500 m m.s.l.) a contrary thermal asymmetry is detected: the western half of the valley cross section results warmer than the eastern one (Fig. 8), suggesting that more intense compensating downward motions is induced here by up-slope flows, developing earlier in the morning along the sun-facing western sidewalls. Such a feature confirms analogous findings by Laiti et al. (2013a) for this area.

5.3.2 Lakes Valley – Spirals B1 and C1

An analogous cross-valley thermal asymmetry is observed for the sections extracted from potential temperature fields regridded around spirals performed further up-valley, i.e. B1 and C1. The downward tilting of the isentropes around 1500 m m.s.l. height (i.e. average crest level) reveals a warmer atmosphere close to the western valley sidewalls, which directly face the sun in the morning hours. This is particularly evident for section B1 (Fig. 10), where a pronounced cross-valley thermal gradient is detected also at lower heights, almost down to the lowest point of the flight trajectory (~ 350 m above the local valley floor height). Accordingly, the nearly N-S orientation of the valley axis turns out to affect to a large extent the thermal structure of the ABL during the morning heating phase. Moreover, the local cross section is very narrow, and the (morning) sun-facing western slopes are steeper and less vegetated than the opposite ones, being partly covered by bare rock; this land cover dissimilarity is likely to enhance the local temperature contrast between the two halves of the valley atmosphere, contributing

ACPD
13, 19121–19171, 2013

to the development of asymmetric slope circulations in the area (notice that a similar pattern was outlined in the area of Cavedine Lake in Laiti et al., 2013b).

5.3.3 Interaction area – Spirals D2 and E2

The analysis of high-resolution potential temperature 3-D fields from the afternoon flight provides some insight also on the flow patterns characterizing the interaction between the *Ora del Garda* and the Adige Valley up-valley wind in the area of the saddle of Terlago, at the Lakes Valley end.

Figure 11 displays the cross-valley thermal structure of the valley atmosphere in the Terlago basin, ~ 2 km up-stream with respect to the saddle ridge: the cooler, denser air, which forms the core of the breeze flow, is shifted to the northwestern half of the valley cross section. This channelling of the up-valley current along the northwestern sidewall is likely to depend on the fact that the valley axis bends eastward a few kilometres down-valley (i.e. up-stream). The *Ora del Garda* main stream is pushed against the external side of this curve (i.e. against the northwestern sidewall) by inertial forces. This phenomenon is similar to some extent to the flow pattern observed by Weigel and Rotach (2004) in the Riviera Valley: they identified a "jet" structure shifted towards the eastern slope at the valley entrance, as a result of the centrifugal acceleration driven by the local valley curvature. In the Lakes Valley, the presence in the area of a more than 200 m high hillock (reported as semi-transparent topography profile in Fig. 11) may contribute to the northward deflection of the lowest atmosphere airflow, which is funnelled towards the lowest point of the Terlago saddle's ridge (indicated by the black arrow in the figure).

On the other hand, spiral E2 (Fig. 12), performed slightly south to this preferential overflow point, reveals that the inlet of the *Ora del Garda* from the Lakes Valley into the underlying Adige Valley produces a complex ABL structure above the floor of the latter. As supported by surface wind observations (see Sect. 5.1.4), the 304.25 and 304.50 K isentropes (which can be roughly considered to represent streamlines) suggest the presence of a strong westerly katabatic current pouring down the saddle of Terlago, flowing down on the Adige Valley bottom, and then impinging on the opposite sidewall. The depth of the layer where an intense turbulent recirculation ensuing from this flow pattern is likely to occur may be estimated in approximately 1300 m (consistently with previous findings summarized in Wagner, 1938), for a sharp potential temperature gradient is found above 1500 m m.s.l. height. This marks the transition to an upper region containing air warmer and drier than at the same height in the Lakes Valley (cf. the difference between the upper parts of E2 and D2 pseudo-soundings; Figs. 6b and 7b). This layer is likely to represent the Adige Valley up-valley flow, displaced to higher heights by the denser air overflowing from the Lakes Valley down to the Adige Valley bottom, accordingly to the findings by Schaller (1936). Previous results by Laiti et al. (2013b) suggest the occurrence of a down-slope jet followed by a "hydraulic jump" flow structure in this area. Actually, features similar to those of "gap flows" conditions described in the Alps by Armi and Mayr (2007), Flamant et al. (2002), Gohm and Mayr (2004) and Mayr et al. (2007) among others, may be identified also in the potential temperature field of Fig. 12: the quasi-vertical pattern of 304.00–305.00 K isentropes (∼ streamlines) in the middle of the valley cross section (between 500 and 1000 m horizontal coordinate) outlines the rebounding of the airflow depth to a higher level than up-stream, i.e. a hydraulic jump. This marks the transition between the strong westerly current, pouring from the Lakes Valley, and a more stagnating flow regime, generated by the obstruction exerted by the eastern Adige Valley sidewall in front of the saddle of Terlago.

6 Conclusions

This study investigated the thermal structure of the lower atmosphere accompanying the development of a coupled lake and valley wind – the *Ora del Garda* – blowing on sunny days from Lake Garda to the Adige Valley in the Alps. The analyses are based on a composite dataset of both surface and airborne observations. The latter were collected by means of an instrumented motorglider on 23 August 2001, when weather

ACPD
13, 19121–19171, 2013

conditions allowed a vigorous development of the investigated thermally-driven circulation. The integration of both surface and airborne observations provided a valuable picture of the complex 3-D thermal field produced by the coupling between the lake breeze and the slope/valley winds, and of the associated valley ABL structures. Residual kriging (RK) technique provided the appropriate tool to characterize the ABL fine-scale variability associated with local circulations developing over complex terrain. Moreover, RK interpolation method presents the advantage of relying on the characteristic covariance of the specific target field; the technique also allows the determination of the characteristic spatial anisotropy of the target field, and efficiently accounts for it. Lastly, RK implementation inherently provides an estimate of the interpolation error.

Time series of observations collected from AWSs disseminated along the valley floor confirmed that the flight day is representative of a "typical" *Ora del Garda* day, and allowed the identification of the different stages of its diurnal cycle. In particular, a well-defined lake breeze front was found to propagate inland from the shoreline, starting at around 10:00 LST. Both surface observations and RK-interpolated field of potential temperature from airborne data (spiral A1) revealed that the morning penetration of the front into the lower Sarca Valley was not homogenous: in fact its propagation across the easternmost part of the basin was found to occur ~ 1.5 h later than in the western half of the basin, which is earlier heated by solar radiation. Stations further up-valley in the Lakes Valley did not show any clear evidence of the passage of a well-defined lake breeze front. However at all of them the surface temperature daily cycle markedly differed from the typical textbook pattern, due to the continuous advection of colder air from above Lake Garda's surface. The average breeze intensity at the shoreline was $\sim 5.5\,\mathrm{m\,s^{-1}}$, with gusts up to $9\,\mathrm{m\,s^{-1}}$, the climax being reached at 14:00 LST at RDG, and one or two hours later in the upper Lakes Valley. The *Ora del Garda* outbreak into the Adige Valley was first detected at 14:00 LST at GAR and at 15:30 LST at RON (this delay being due to the more sheltered position of RON with respect to GAR); the westerly inflow of air from the Lakes Valley continued until the late evening (21:00 LST), being particularly intense in the late afternoon hours, with gusts up to $11.3\,\mathrm{m\,s^{-1}}$ at

ACPD
13, 19121–19171, 2013

the Adige Valley floor. Indeed, at 19:00 LST the *Ora del Garda* airflow channelling in southward direction along the Adige Valley even reached TNS station about 5 km south of Trento city, overwhelming the regular up-valley wind formerly recorded in the area (average intensity: $\sim 2.5\,\mathrm{m\,s^{-1}}$).

Associated with the *Ora del Garda* development, a characteristic ABL structure was observed in the lower Sarca Valley and in the Lakes Valley: rather shallow MLs, displaying depths in the order of 500 m, developed over the valley floor, surmounted by slightly stable layers and/or elevated QMLs, extending almost up to the sidewall-crest heights (~ 1500 m m.s.l.). This characteristic ABL pattern is determined by the development of up-slope winds during the morning heating phase, whose compensation flows cause the local subsidence of the potentially warmer, stable mid-valley air from the free atmosphere (Kuwagata and Kimura, 1995, 1997; Rampanelli et al., 2004; Serafin and Zardi, 2010a,b, 2011). 3-D high-resolution potential temperature fields highlighted that in the lower Lakes Valley (spiral B1), due to the roughly S–N valley orientation, and to local differences in the land cover of lateral slopes, the local subsidence associated with morning heating was much more intense close to the sunlit western sidewalls than to the eastern ones, and induces pronounced cross-valley thermal asymmetries. Moreover, the ML depth and its mean potential temperature θ_m gradually increased up-slope along the valley axis from Lake Garda's shoreline to the valley end. As expected, θ_m grew also with time, but not as fast as in the nearby Adige Valley. The limiting factor is the up-valley advection of colder air from above the Lake Garda's surface operated by the *Ora del Garda*, which suppresses the temperature rise in the lowest valley atmosphere and further inhibits the convective ML growth, stabilizing the profile down to very low height, especially close to the lake's shoreline.

Concerning the daily evolution of the ABL structure, the comparison between pseudo-soundings from flights #1 and #2 for D and E sites provided an interesting picture for the area where the two local airflows interact. In the late morning unstable surface layers surmounted by ~ 500 m deep MLs were detected in this area and also further down-valley (i.e. at A, B and C sites), while in the afternoon the ML depth re-

ACPD
13, 19121–19171, 2013

sulted consistently increased at E site, as its vertical extent had almost tripled (from 400 to 1200 m). On the contrary, the ML depth at D site was slightly reduced between the morning and the afternoon (from 750 to 600 m). Moreover, afternoon observations from local surface stations revealed the establishment of neutrally- or stably-stratified surface layers (respectively at D and E sites). This suggests that, differently from the morning, in the afternoon the surface sensible heat fluxes are no more sustaining the convective growth of the ML in the area. As this transition occurs before sunset, it cannot be induced by the radiative cooling of the ground surface. On the contrary, it is consistent with the cold air advection and the strong ventilation at the lowest levels operated by the *Ora del Garda*.

As anticipated, in the afternoon the *Ora del Garda* breaks out into the Adige Valley from the saddle of Terlago on its western sidewall, and produces an intense katabatic flow in the area, with potentially cooler air rapidly descending down the underlying valley floor. RK-mapping for spiral D2 suggested that at the Lakes Valley end the *Ora del Garda* channels preferentially along the northwestern sidewall of the valley towards the lowest point of the Terlago saddle ridge, due to the local eastward curvature of the valley and to the inertia of the intense up-valley flow. On the other hand, the thermal structure in the Adige Valley (emerging from spiral E2) displayed conditions similar to those of a "gap flow" developing across the Terlago saddle, followed by a hydraulic jump further down-stream, due to the blocking by the opposite valley sidewall. The depth of this down-stream layer, where an intense turbulent recirculation occurs, was of about 1300 m. Actually, the above-mentioned deepening of the ML in the Adige Valley from ~ 400 m to ~ 1200 m, occurring approximately between 12:00 and 15:00 LST, was likely produced by the strong mechanical mixing following the *Ora del Garda* outbreak rather than by a CBL growth driven by surface sensible heat fluxes. This picture is consistent with previous investigations by Schaller (1936), de Franceschi et al. (2002) and others (reported in Wagner, 1938); accordingly, the warmer and drier air mass found above this deep ML may be identified with the local up-valley flow (whose regular development

ACPD
13, 19121–19171, 2013

is hindered by the *Ora del Garda* overflow), being displaced at higher heights by the denser wedge of potentially cooler air that forms at the Adige Valley bottom.

All of the above findings are consistent with previous results contained in Laiti et al. (2013a,b). The present work adds further information to the understanding of the *Ora del Garda* low-level circulation and ABL pattern, in particular for what concerns the lake-breeze front penetration in the shoreline area in the late morning and the evolution of the thermal structure of the atmosphere at the junction between the Lakes Valley and the Adige Valley. However, these two key aspects of the *Ora del Garda* circulation system will be fully investigated only by performing additional targeted measurement campaigns, or by carrying out high-resolution numerical simulations for the area, which we intend to perform in the next future. Indeed, RK-interpolated meteorological fields inherently provide a degree of spatial detail that is comparable to the resolution of LES simulations explicitly resolving ABL structures associated to thermally-driven winds (Antonelli and Rotunno, 2007; Catalano and Cenedese, 2010; Catalano and Moeng, 2010; Chow et al., 2006; Crosman and Horel, 2012; Lehner and Whiteman, 2012; Serafin and Zardi, 2010a,b, 2011; Weigel et al., 2006). Accordingly, RK results represent a valuable basis for the validation of high-resolution modelling results. Finally, RK analyses of airborne measurements will in general be useful for achieving a more complete understanding of typical ABL processes affecting air quality (Palau et al., 2005; Gohm et al., 2009), turbulent fluxes (Druilhet and Durand, 1997; de Franceschi et al., 2009), urban weather and climate (Giovannini et al., 2011, 2013a,b), and even atmospheric convection leading to precipitation events (Bertò et al., 2004; Eigenmann et al., 2009; Pucillo et al., 2009) in complex terrain environments.

Acknowledgements. The Authors would like to thank the Trento University Sport Centre (CUS Trento) for providing the motorglider, and the pilot, Fabrizio Interlandi, for performing the flights. Meteorological observations from surface weather stations and radiosoundings were provided by the GIS and Remote Sensing Unit of the Edmund Mach Foundation, the Meteorological Office of the Autonomous Province of Trento (Meteotrentino) and the Meteorological Office of the Italian Air Force. Radiosoundings were also downloaded from the University of Wyoming website.

References

Ahmed, S. and de Marsily, G.: Comparison of geostatistical methods for estimating transmissivity using data on transmissivity and specific capacity, Water Resour. Res., 23, 1717–1737, 1987.

Antonelli, M. and Rotunno, R.: Large-Eddy Simulation of the Onset of the Sea Breeze, J. Atmos. Sci., 64, 4445–4457, 2007.

Armi, L. and Mayr, G. J.: Continuously stratified flows across an Alpine crest with a pass: shallow and deep föhn, Q. J. Roy. Meteor. Soc., 133, 459–477, 2007.

Atkinson, B. W.: Mesoscale atmospheric circulation, Academic Press, London, 494 pp, 1981.

Baldi, M., Cesari, R., Tampieri, F., Tranquillini, M., and Zardi, D.: A study of the valley wind known as Ora del Garda. Civil and Environmental Engineering Department Tech, Note IDR 1/1999, University of Trento, Trento, Italy, 119 pp., 1999.

Bastin, S., Drobinski, P., Dabas, A., Delville, P., Reitebuch, O., and Werner, C.: Impact of the Rhône and Durance valleys on sea-breeze circulation in the Marseille area, Atmos. Res., 74, 303–328, 2005.

Bergström, H. and Juuso, N.: A study of valley winds using the MIUU meso-scale model, Wind Energy, 6, 109–129, 2006.

Bertò, A., Buzzi, A., and Zardi, D.: Back-traking water vapour contributing to precipitation event over Trentino: a case study, Meteorol. Z., 13, 189–200, 2004.

Boybeyi, Z. and Raman., S.: A three-dimensional numerical sensitivity study of mesoscale circulations induced by circular lakes, Meteorol. Atmos. Phys., 49, 19–41, 1992

Boyouk, N., Léon, J. F., Delbarre, H., Augustin, P., and Fourmentin, M.: Impact of sea breeze on vertical structure of aerosol optical properties in Dunkerque, France, Atmos. Res., 101, 902–910, 2011.

Carroll, J. J. and Baskett, R. L.: Dependence of air quality in a remote location on local and mesoscale transports: a case study, J. Appl. Meteorol., 18, 474–486, 1979.

Catalano, F. and Cenedese, A.: High-resolution numerical modeling of thermally driven slope winds in a valley with strong capping, J. Appl. Meteorol. Clim., 49, 1859–1880, 2010.

Catalano, F. and Moeng, C. H.: Large-eddy simulation of the daytime boundary layer in an idealized valley using the weather research and forecasting numerical model, Bound.-Lay. Meteorol., 137, 49–75, 2010.

Chow, F. K., Weigel, A. P., Street, R. L., Rotach, M. W., and Xue, M.: High-resolution large-eddy simulations of flow in a steep Alpine valley, Part I: Methodology, verification, and sensitivity experiments, J. Appl. Meteorol. Clim., 45, 63–86, 2006.

Cressie, N. A. C.: Statistics for Spatial Data, revised edn., John Wiley and Sons, New York, 900 pp., 1993.

Crosman, E. and Horel, J.: Sea and Lake Breezes: a review of numerical studies, Bound.-Lay. Meteorol., 137, 1–29, 2010.

Crosman, E. and Horel, J.: Idealized Large-Eddy simulations of sea and Lake Breezes: sensitivity to Lake Diameter, heat flux and stability, Bound.-Lay. Meteorol., 144, 309–328, 2012.

Daves, B., Tampieri, F., Tubino, M., and Zardi, D.: Exchange processes in a valley system: the effects of local circulation, in: Proc. 25th International Conference on Alpine Meteorology, Turin, Italy, 1998.

de Franceschi, M.: Investigation of Atmospheric Boundary Layer Dynamics in Alpine Valleys, Ph.D. thesis, University of Trento, Trento, Italy, 2004.

de Franceschi, M. and Zardi, D.: Evaluation of cut-off frequency and correction of filter-induced phase lag and attenuation in eddy covariance analysis of turbulence data, Bound.-Lay. Meteorol., 108, 289–303, 2003.

de Franceschi, M., Rampanelli, G., and Zardi, D.: Further investigations of the Ora del Garda valley wind, Preprints, 10th Conference on Mountain Meteorology and MAP Meeting 2002, Park City, UT, 2002.

de Franceschi, M., Rampanelli, G., Sguerso, D., Zardi, D., and Zatelli, P.: Development of a measurement platform on a light airplane and analysis of airborne measurements in the atmospheric boundary layer, Ann. Geophys., 46, 269–283, 2003, http://www.ann-geophys.net/46/269/2003/.

de Franceschi, M., Zardi, D., Tagliazucca, M., and Tampieri, F.: Analysis of second order moments in the surface layer turbulence in an Alpine valley, Q. J. Roy. Meteor. Soc., 135, 1750–1765, 2009.

De Wekker, S. F. J.: Structure and Morphology of the Convective Boundary Layer in Mountainous Terrain, PhD dissertation, University of British Columbia, BC, Canada, 191 pp., 2002.

De Wekker, S. F. J., Steyn, D. G., and Nyeki, S.: A comparison of aerosol-layer and convective boundary-layer structure over a mountain range during Staaarte '97, Bound.-Lay. Meteorol., 113, 249–271, 2004.

ACPD
13, 19121–19171, 2013

Analysis of the *Ora del Garda* wind from airborne measurements

L. Laiti et al.

Defant, A.: Berg- und Talwinde in Südtirol (Mountain and valley winds in southern Tyrol), S. B. Akad. Wiss. Wien, 118, 553–604, 1909.
Defant, F.: Local winds, in: Compendium of Meteorology, edited by: Malone, T. F., Amer. Meteor. Soc., 655–672, 1951.
Drobinski, P., Saïd, F. F., Ancellet, G., Arteta, J., Augustin, P., Bastin, S., Brut, A., Caccia, J., Campistron, B., Cautenet, S., Colette, A., Coll, I., Corsmeier, U., Cros, B., Dabas, A., Delbarre, H., Dufour, A., Durand, P., Guénard, V., Hasel, M., Kalthoff, N., Kottmeier, C., Lasry, F., Lemonsu, A., Lohou, F., Masson, V., Menut, L., Moppert, C., Peuch, V., Puygrenier, V., Reitebuch, O., and Vautard, R.: Regional transport and dilution during high-pollution episodes in southern France: summary of findings from the field Experiment to Constraint Models of Atmospheric Pollution and Emissions Transport (ESCOMPTE), J. Geophys. Res., 112, D13105, doi:10.1029/2006JD007494, 2007.
Druilhet, A. and Durand, P.: Experimental investigation of atmospheric boundary layer turbulenc, Atmos. Res., 43, 345–388, 1997.
Egger, J.: Pressure distributions in the Dischma Valley during the field experiment DISKUS, Contrib. Atmos. Phys., 56, 163–176, 1983.
Eigenmann, R., Metzger, S., and Foken, T.: Generation of free convection due to changes of the local circulation system, Atmos. Chem. Phys., 9, 8587–8600, doi:10.5194/acp-9-8587-2009, 2009.
Finkele, K., Hacker, J. M., Kraus, H., and Byron-Scott, R. A. D.: A complete sea-breeze circulation cell derived from aircraft observations, Bound.-Lay. Meteorol., 73, 299–317, 1995.
Flamant, B. C., Drobinski, P., Nance, L., Banta, R., Darby, L., and Dusek, J.: Gap flow in an Alpine valley during a shallow south föhn event: observations, numerical simulations and hydraulic analogue, Q. J. Roy. Meteor. Soc., 128, 1173–1210, 2002.
Giovannini, L.: Urban scale phenomena and boundary layer processes in mountain valleys, Ph.D. thesis, University of Trento, Trento, Italy, 2012.
Giovannini, L., Zardi, D., and de Franceschi, M.: Analysis of the Urban Thermal Fingerprint of the City of Trento in the Alps, J. Appl. Meteorol. Clim., 50, 1145–1162, 2011.
Giovannini, L., Zardi, D., and de Franceschi, M.: Characterization of the thermal structure inside an urban canyon: field measurements and validation of a simple model, J. Appl. Meteorol. Clim., 52, 64–81, 2013a.

ACPD
13, 19121–19171, 2013

Giovannini, L., Zardi, D., de Franceschi, M., and Chen, F.: Numerical simulations of boundary-layer processes and urban-induced alterations in an Alpine valley, Int. J. Climatol., doi:10.1002/joc.3750, in press, 2013b.
Gohm, A. and Mayr, G. J.: Hydraulic aspects of föhn winds in an Alpine valley, Q. J. Roy. Meteor. Soc., 130, 449–480, 2004.
Gohm, A., Harnisch, F., Vergeiner, J., Obleitner, F., Schnitzhofer, R., Hansel, A., Fix, A., Neininger, B., Emeis, S., and Schäfer, K.: Air pollution transport in an Alpine valley: results from airborne and ground-based observations, Bound.-Lay. Meteorol., 131, 441–463, 2009.
Goovaerts, P.: Geostatistics for natural resources evaluation, Oxford University Press, New York, 483 pp., 1997.
Goovaerts, P.: Using elevation to aid the geostatistical mapping of rainfall erosivity, Catena, 34, 227–242, 1999.
Harnisch, F., Gohm, A., Fix, A., Schnitzhofer, R., Hansel, A., and Neininger, B.: Spatial distribution of aerosols in the Inn Valley atmosphere during wintertime, Meteorol. Atmos. Phys., 103, 223–235, 2009.
Hasel, M., Kottmeier, C., Corsmeier, U., and Wieser, A.: Airborne measurements of turbulent trace gas fluxes and analysis of eddy structure in the convective boundary layer over complex terrain, Atmos. Res., 74, 381–402, 2005.
Hennemuth, B.: Temperature field and energy budget of a small Alpine valley, Contrib. Atmos. Phys., 58, 545–559, 1985.
Hennemuth, B.: Thermal asymmetry and cross-valley circulation in a small Alpine valley, Bound.-Lay. Meteorol., 36, 371–394, 1986.
Hennemuth, B. and Schmidt, H.: Wind phenomena in the Dischma Valley during DISKUS, Arch. Meteor. Geophys. Bioklimatol., B35, 361–387, 1985.
Kalthoff, N., Adler, B., Barthlott, C., Corsmeier, U., Mobbs, S., Crewell, S., Träumner, K., Kottmeier, C., Wieser, A., Smith, V., and Di Girolamo, P.: The impact of convergence zones on the initiation of deep convection: a case study from COPS, Atmos. Res., 93, 680–694, 2009.
Keen, C. S. and Lyons, W. A.: Lake/land breeze circulations on the western shore of Lake Michigan, J. Appl. Meteorol., 1843–1855, 1978.
Kitada, T., Igarashi, K., and Owada, M.: Numerical-analysis of air-pollution in a combined field of land sea breeze and mountain valley wind, J. Climate Appl. Meteorol., 25, 767–784, 1986.

ACPD
13, 19121–19171, 2013

Analysis of the *Ora del Garda* wind from airborne measurements

L. Laiti et al.

Kondo, H.: A Numerical experiment of the “Extended Sea Breeze” over the Kanto Plain, J. Meteorol. Soc. Jpn., 68, 419–434, 1990a.
Kondo, H.: A numerical experiment on the interaction between sea breeze and valley wind to generate the so-called “Extended Sea Breeze”, J. Meteorol. Soc. Jpn., 68, 435–446, 1990b.
Kossmann, M., Sturman, A. P., Zawar-Reza, P., McGowan, H. A., Oliphant, A. J., Owens, I. F., and Spronken-Smith, R. A.: Analysis of the wind field and heat budget in an Alpine lake basin during summertime fair weather conditions, Meteorol. Atmos. Phys., 81, 27–52, 2002.
Kraus, H., Hacker, J. M., and Hartmann, J.: An observational aircraft-based study of the breeze frontogenesis, Bound.-Lay. Meteorol., 53, 223–265, 1990.
Kuwagata, T. and Kimura, F.: Daytime boundary layer evolution in a deep valley, Part I: Observations in the Ina Valley, J. Appl. Meteorol., 34, 1082–1091, 1995.
Kuwagata, T. and Kimura, F.: Daytime boundary layer evolution in a deep valley, Part II: Numerical simulation of the cross-valley circulation, J. Appl. Meteorol., 36, 883–895, 1997.
Laiti, L., Zardi, D., de Franceschi, M., and Rampanelli, G.: Residual Kriging analysis of airborne measurements: application to the mapping of atmospheric boundary-layer thermal structures in a mountain valley, Atmos. Sci. Lett., 14, 79–85, 2013a.
Laiti, L., Zardi, D., de Franceschi, M., and Rampanelli, G.: Atmospheric boundary-layer structures associated with the *Ora del Garda* wind in the Alps as revealed from airborne and surface measurements, Atmos. Res., doi:10.1016/j.atmosres.2013.07.006, 2013b.
Lehner, M. and Whiteman, C. D.: The thermally driven cross-basin circulation in idealized basins under varying wind conditions, J. Appl. Meteorol. Clim., 51, 1026–1045, 2012.
Lu, R. and Turco, R. P.: Air pollutant transport in a coastal environment, Part I: Two-dimensional simulations of sea-breeze and mountain effects, J. Atmos. Sci., 51, 2285–2308, 1994.
Lu, R. and Turco, R. P.: Air pollutant transport in a coastal environment, Part II: Three-dimensional simulations over Los Angeles basin, Atmos. Environ., 29, 1499–1518, 1995.
Lyons, W. A. and Olsson, L. E.: Detailed Mesometeorological studies of air pollution dispersion in the Chicago Lake Breeze, Mon. Weather Rev., 101, 387–403, 1973.
Mahrer, Y. and Pielke, R. A.: The effects of topography on sea and land breezes in a two-dimensional numerical model, Mon. Weather Rev., 105, 1151–1162, 1977.
Mayr, G. J., Laurence, A., Gohm, A., Zängl, G., Durran, D. R., Flamant, C., Gaberšek, S., Mobbs, S., Ross, A., and Weissmann, M.: Gap flows: results from the mesoscale Alpine programme, Q. J. Roy. Meteor. Soc., 133, 881–896, 2007.

ACPD
13, 19121–19171, 2013

McGowan, H. A. and Sturman, A. P.: Interacting multi-scale wind systems within an Alpine basin, Lake Tekapo, New Zealand, Meteorol. Atmos. Phys., 58, 165–177, 1996.
McGowan, H. A., Owens, I. F., and Sturman, A. P.: Thermal and dynamic characteristics of Alpine lake breezes, Lake Tekapo, New Zealand, Bound.-Lay. Meteorol., 76, 3–24, 1995.
Neumann, J. and Mahrer, Y.: A theoretical study of the lake and land breezes of circular lakes, Mon. Weather Rev., 103, 474–485, 1975.
Odeh, I. O. A., McBratney, A. B., and Chittleborough, D. J.: Spatial prediction of soil properties from landform attributes derived from a digital elevation model, Geoderma, 63, 197–214, 1994.
Odeh, I. O. A., McBratney, A. B., and Chittleborough, D. J.: Further results on prediction of soil properties from terrain attributes: heterotropic cokriging and regression-kriging, Geoderma, 67, 215–22, 1995.
Palau, J. L., Pérez-Landa, G., Diéguez, J. J., Monter, C., and Millán, M. M.: The importance of meteorological scales to forecast air pollution scenarios on coastal complex terrain, Atmos. Chem. Phys., 5, 2771–2785, doi:10.5194/acp-5-2771-2005, 2005.
Pérez-Landa, G., Ciais, P., Gangoiti, G., Palau, J. L., Carrara, A., Gioli, B., Miglietta, F., Schumacher, M., Millán, M. M., and Sanz, M. J.: Mesoscale circulations over complex terrain in the Valencia coastal region, Spain – Part 2: Modeling CO_2 transport using idealized surface fluxes, Atmos. Chem. Phys., 7, 1851–1868, doi:10.5194/acp-7-1851-2007, 2007.
Pielke, R. A.: Mesoscale meteorological modeling, 1st edn., Academic Press, New York, 612 pp., 1984.
Pollak, L. W.: Berg- und Talwinde im Becken von Trient [The wind directions in Trento basin], Meteor. Z., 41, 18–21, 1924.
Pucillo, A., Giaiotti, D. B., and Stel, F.: Ground wind convergence as source of deep convection initiation, Atmos. Res., 93, 437–445, 2009.
Puygrenier, V., Lohou, F., Campistron, B., Saïd, F., Pigeon, G., Bénech, B., and Serça, D.: Investigation of the fine structure of sea-breeze during ESCOMPTE experiment, Atmos. Res., 74, 329–353, 2005.
Rampanelli, G., Zardi, D., and Rotunno, R.: Mechanisms of up-valley winds, J. Atmos. Sci., 61, 3097–3111, 2004.
Rotach, M. W. and Zardi, D.: On the boundary layer structure over highly complex terrain: key findings from MAP, Q. J. Roy. Meteor. Soc., 133, 937–948, 2007.

Schaller, E.: Aerologische Untersuchung des periodischen Talwindsystems von Trient (Aerologic investigation of the periodic valley wind system of Trento), Dissertation, Innsbruck, 1936.
Schnitzhofer, R., Norman, M., Wisthaler, A., Vergeiner, J., Harnisch, F., Gohm, A., Obleitner, F., Fix, A., Neininger, B., and Hansel, A.: A multimethodological approach to study the spatial distribution of air pollution in an Alpine valley during wintertime, Atmos. Chem. Phys., 9, 3385–3396, doi:10.5194/acp-9-3385-2009, 2009.
Segal, M., Leuthold, M., Arritt, R. W., Anderson, C., and Shen, J.: Small lake daytime breezes: some observational and conceptual evaluations, B. Am. Meterol. Soc., 78, 1135–1147, 2007.
Serafin, S. and Zardi, D.: Structure of the atmospheric boundary layer in the vicinity of a developing up-slope flow system: a numerical model study, J. Atmos. Sci., 67, 1171–1185, 2010a.
Serafin, S. and Zardi, D.: Daytime heat transfer processes related to slope flows and turbulent convection in an idealized mountain valley, J. Atmos. Sci., 67, 3739–3756, 2010b.
Serafin, S. and Zardi, D.: Daytime development of the boundary layer over a plain and in a valley under fair weather conditions: a comparison by means of idealized numerical simulations, J. Atmos. Sci., 68, 2128–2141, 2011.
Sills, D. M. L., Brook, J. R., Levy, I., Makar, P. A., Zhang, J., and Taylor, P. A.: Lake breezes in the southern Great Lakes region and their influence during BAQS-Met 2007, Atmos. Chem. Phys., 11, 7955–7973, doi:10.5194/acp-11-7955-2011, 2011.
Simpson, J. E.: Sea breeze and local winds, Cambridge University Press, Cambridge, 234 pp., 1994.
Stephan, K., Kraus, H., Ewenz, C. M., and Hacker, J. M.: Sea-breeze front variations in space and time, Meteorol. Atmos. Phys., 70, 81–95, 1999.
Stull, R. B.: An Introduction to Boundary Layer Meteorology, Kluwer Academic, 666 pp., 1988.
Wagner, A.: Theorie und Beobachtung der periodischen Gebirgswinde (Theory and observation of periodic mountain winds), Gerlands Beitr. Geophys., 52, 408–449, 1938, English translation: Whiteman, C. D. and Dreiseit, E.: Alpine Meteorology: Translations of Classic Contributions, edited by: Wagner, A., Ekhart, E., and Defant, F., PNL-5141/ASCOT-84-3, Pacific Northwest Laboratory, Richland, Washington, 121 pp., 1984
Wakimoto, R. M. and McElroy, J. L.: Lidar observation of elevated pollution layers over Los Angeles, J. Appl. Meteorol. Clim., 25, 1583–1599, 1986.

ACPD
13, 19121–19171, 2013

Weigel, A. P. and Rotach, M. W.: Flow structure and turbulence characteristics of the daytime atmosphere in a steep and narrow Alpine valley, Q. J. Roy. Meteor. Soc., 130, 2605–2627, 2004.

Weigel, A. P., Chow, F. K., Rotach, M. W., Street, R. L., and Xue, M.: High-resolution large-eddy simulations of flow in a steep Alpine valley, Part II: Flow structure and heat budgets, J. Appl. Meteorol. Clim., 45, 87–107, 2006.

Weigel, A. P., Chow, F. K., and Rotach, M. W.: The effect of mountainous topography on moisture exchange between the "surface" and the free atmosphere, Bound.-Layer Meteorol., 125, 227–244, 2007.

Wiener, V.: Die Windrichtungen im Becken von Trient [The wind directions in Trento basin], Dissertation, Prague, 1929.

Wood, R., Stromberg, I. M., and Jonas, P. R.: Aircraft observations of sea-breeze frontal structure, Q. J. Roy. Meteor. Soc., 125, 1959–1995, 1999.

Zardi, D. and Whiteman, C. D.: Diurnal mountain wind systems, in: Mountain Weather Research and Forecasting: Recent Progress and Current Challenges, edited by: Chow, F. K., De Wekker, S. F. J., and Snyder, B., Springer, 35–119, 2013.

Zardi, D., Gerola, R., Tampieri, F., and Tubino, M.: Measurement and modelling of a valley wind system in the Alps, in: Proc. 13th Symp. on Boundary Layers and Turbulence, Dallas, TX, Amer. Meteorol. Soc, 28–31, 1999.

Zumpfe, D. E. and Horel., J. D.: Lake-Breeze Fronts in the Salt Lake Valley, J. Appl. Meteorol. Clim., 46, 196–211, 2007.

ACPD

13, 19121–19171, 2013

Table 1. Timings and characteristics of flights #1 and #2. Single spirals are labelled according to Fig. 2. "CV" and "AV" respectively indicate whether the trajectory explored a cross- or an along-valley oriented section. "D" stands for a descending (downward) flight leg and "U" for an ascending (upward) flight leg.

Flight	Take-off	Landing	Spiral	Start	End	Trajectory
#1	09:00 LST	12:00 LST	E1a	09:18 LST	09:47 LST	CV U
			A1	09:59 LST	10:42 LST	C+AV U+D
			B1	10:46 LST	11:06 LST	CV U
			C1	11:08 LST	11:21 LST	CV D
			D1	11:23 LST	11:43 LST	[–] U
			E1b	11:43 LST	11:57 LST	[–] D
#2	14:15 LST	15:30 LST	E2	14:24 LST	14:54 LST	CV U
			D2	14:58 LST	15:17 LST	CV D

ACPD
13, 19121–19171, 2013

Analysis of the *Ora del Garda* wind from airborne measurements

L. Laiti et al.

Table 2. List of the surface AWSs considered in the study, named and grouped by geographic area as in Fig. 2. Operating institution: "IASMA" stands for Istituto Agrario di San Michele all'Adige, "Meteot." stands for the Meteorological Office of the Autonomous Province of Trento, "APG" stands for Trento University Atmospheric Physics Group. Local terrain height and height of the anemometer (when present) are also reported. ([a]) indicates anemometers recording only wind speed. ([b]) indicates the ultrasonic anemometer operated by the APG.

Group	Station	Institution	Terrain height	Time resolution	Anemometer
a	RDG	IASMA	69 m m.s.l.	1 h	5 m a.g.l.
	TOR	Meteot.	70 m m.s.l.	15 min	[–]
	NAG	IASMA	223 m m.s.l.	1 h	[–]
	TEN	Meteot.	405 m m.s.l.	15 min	[–]
	ARC	Meteot.	91 m m.s.l.	15 min	[–]
	DRO	IASMA	113 m m.s.l.	1 h	[–]
b	CAV	Meteot.	245 m m.s.l.	15 min	[–]
	PIE	IASMA	242 m m.s.l.	1 h	3 m m.s.l.([a])
	MAS	Meteot.	245 m m.s.l.	15 min	[–]
	TER	IASMA	428 m m.s.l.	1 h	3 m m.s.l.([a])
	Monte Terlago	APG	720 m m.s.l.	10 min	3 m m.s.l.
c	TNS	IASMA	185 m m.s.l.	1 h	10 m m.s.l.
	ROM	IASMA	184 m m.s.l.	1 h	[–]
	ALD	IASMA	183 m m.s.l.	1 h	3 m m.s.l.([a])
	BES	IASMA	180 m m.s.l.	1 h	3 m m.s.l.([a])
	VOL	IASMA	175 m m.s.l.	1 h	[–]
	ROV	IASMA	170 m m.s.l.	1 h	3 m m.s.l.([a])
d	RON	Meteot.	194 m m.s.l.	15 min	10 m m.s.l.
	GAR	IASMA	197 m m.s.l.	1 h	3 m m.s.l.
	ZAM	IASMA	201 m m.s.l.	1 h	3 m m.s.l.([a])
	SMA	Meteot.	205 m m.s.l.	15 min	[–]
	Roncafort	APG	200 m m.s.l.	0.04 s	6.5 m m.s.l.([b])

ACPD
13, 19121–19171, 2013

Table 3. Key parameters of the ABL stratification for each valley section explored by flights #1 and #2. Cf. Table 1 and Fig. 2 for the labels of associated flight spirals.

Spiral	Valley floor height	ML depth	θ_m
E1a	195 m m.s.l.	200 m	296.15 K
A1	70 m m.s.l.	200 m	298.45 K
B1	130 m m.s.l.	470 m	300.35 K
C1	245 m m.s.l.	400 m	300.70 K
D1	450 m m.s.l.	750 m	301.80 K
E1b	195 m m.s.l.	400 m	300.55 K
E2	195 m m.s.l.	1200 m	304.00 K
D2	450 m m.s.l.	600 m	303.60 K

ACPD
13, 19121–19171, 2013

Analysis of the *Ora del Garda* wind from airborne measurements

L. Laiti et al.

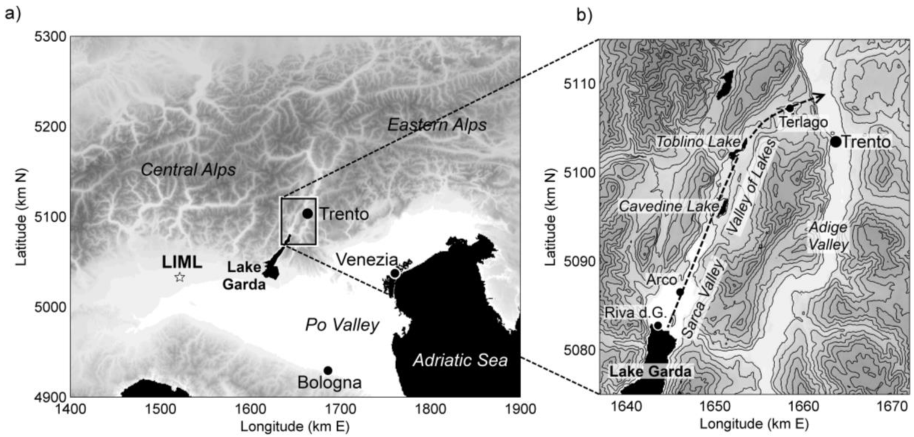

Fig. 1. **(a)** Localization of the study area (rectangular box) near the city of Trento in the south-eastern Italian Alps; Lake Garda and LIML sounding station are also indicated. **(b)** Topography of the target area (contour interval: 200 m); the dashed arrow represents the path of the *Ora del Garda* along the lower Sarca Valley and Lakes Valley, from Lake Garda's northern shoreline to the saddle of Terlago, and, finally, the Adige Valley. Gauss Boaga reference system, Italy East fuse.

ACPD
13, 19121–19171, 2013

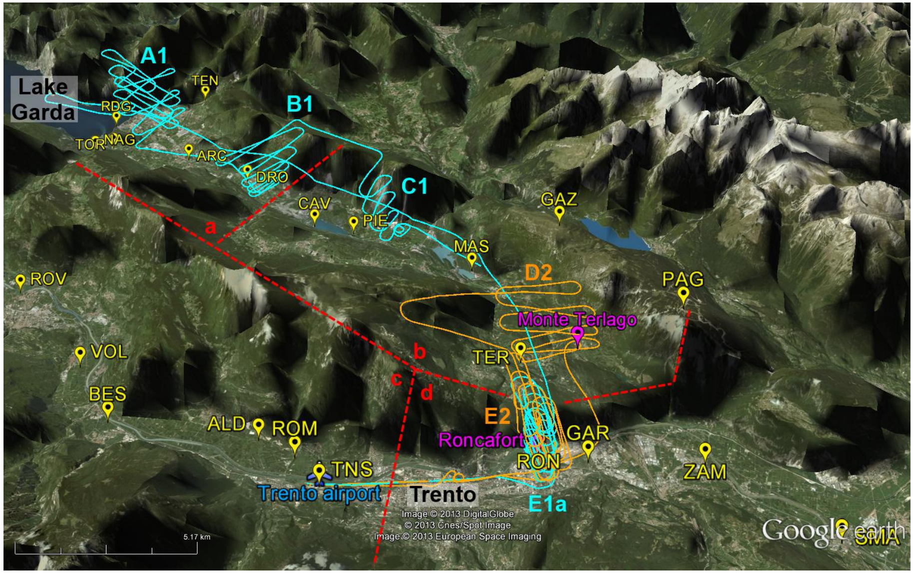

Fig. 2. Cyan line: flight #1 trajectory; orange line: flight #2 trajectory. The names of the single valley sections explored are indicated in correspondent colour (see Table 1; notice that no coordinate data are available for spirals D1 and E1b). Locations of routinely operated AWSs are shown by yellow place-marks (see Table 2). Magenta place-marks indicate the sites where intensive surface measurements were performed. The four geographic areas considered in surface data analysis are also delimited (red dashed lines; see Table 2). View is from E. Background image: ©2013 Google Earth, ©2013 DigitalGlobe, ©2013 Cnes/Spot Image, ©2013 European Space Imaging.

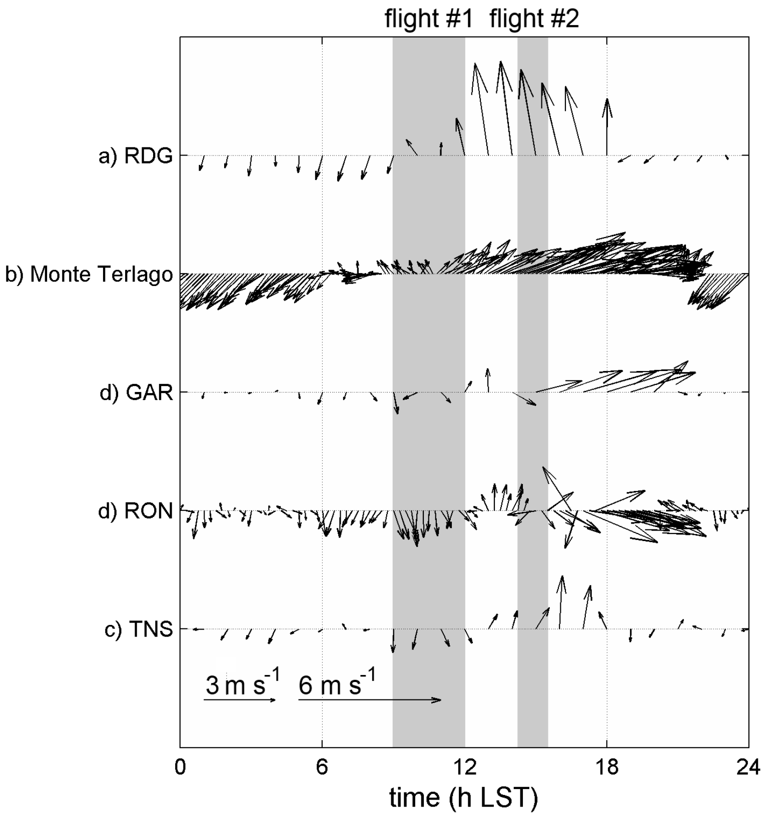

Fig. 3. Wind surface observations (vectors) for 23 August 2001 at RDG (5 m a.g.l. anemometer; averaging interval: 1 h) in the lower Sarca Valley (group a), Monte Terlago (3 m a.g.l.; 10 min) at the end of the Lakes Valley (group b), GAR (3 m a.g.l.; 1 h) and RON (10 m a.g.l.; 15 min) in the Adige Valley north of Trento (group d), and TNS (10 m a.g.l.; 1 h) in the Adige Valley south of Trento (group c). See Table 2 and Fig. 2 for names and locations of the AWSs.

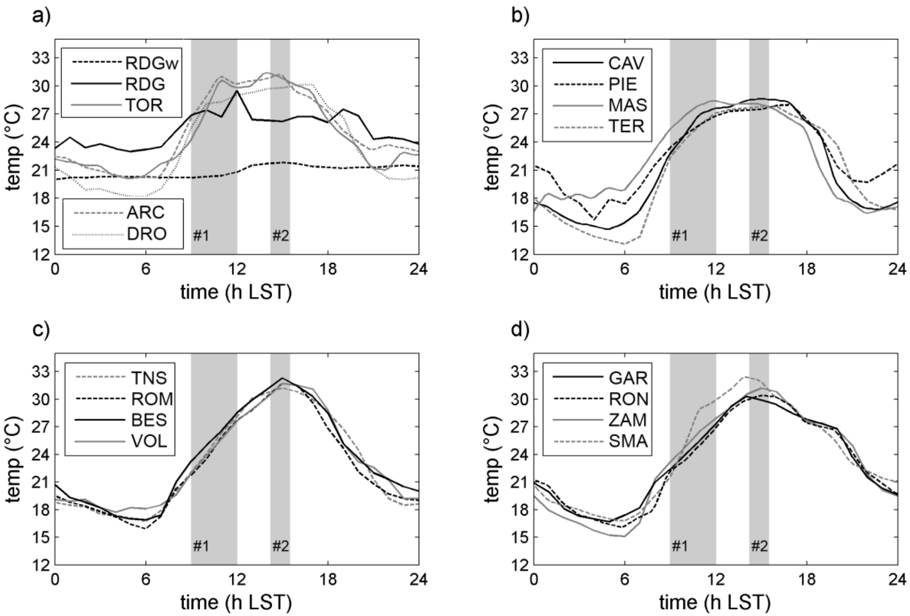

Fig. 4. 2 m a.g.l. air temperature observations from AWSs for 23 August 2001, grouped by geographic area: **(a)** lower Sarca Valley (RDGw indicates lake water temperature measurements at RDG station); **(b)** Lakes Valley; **(c)** Adige Valley, south of Trento; **(d)** Adige Valley, north of Trento. See Table 2 and Fig. 2 for names and locations of the AWSs. The duration of flights #1 and #2 is indicated by the grey bands.

ACPD
13, 19121–19171, 2013

Analysis of the *Ora del Garda* wind from airborne measurements

L. Laiti et al.

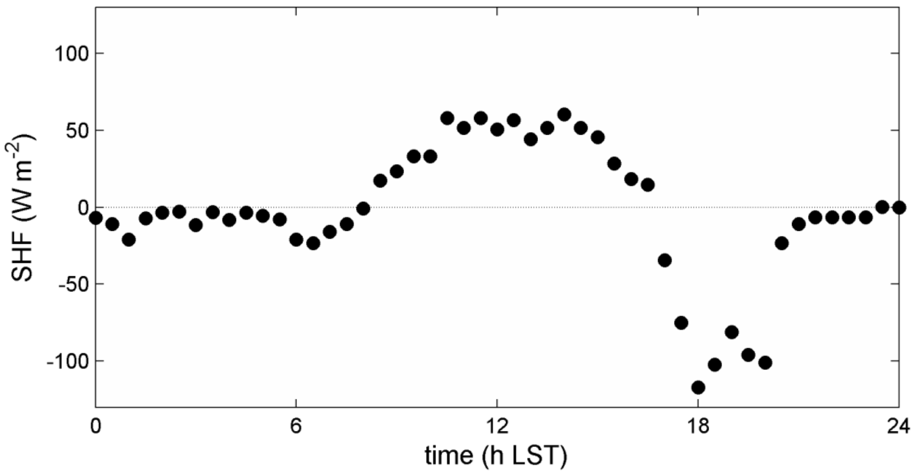

Fig. 5. Time series of vertical sensible heat flux (SHF) for 23 August 2001 from eddy covariance analysis of ultrasonic anemometer measurements (averaging interval: 30 min) collected at Roncafort site (see Fig. 2).

ACPD
13, 19121–19171, 2013

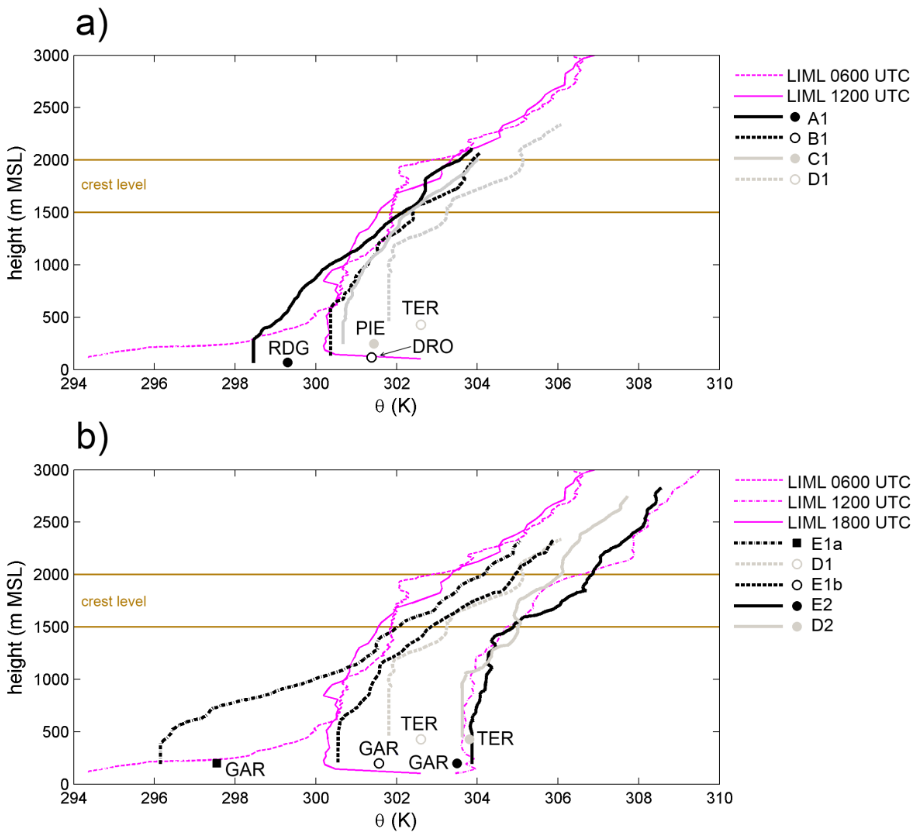

Fig. 6. Potential temperature pseudo-soundings extracted from airborne data (cf. Table 1). **(a)** displays vertical profiles for sites A, B, C and D (Sarca and Lakes valleys) from flight #1. **(b)** shows vertical profiles for sites D and E (i.e. interaction area) from both flights. Associated surface observations from the closest AWSs are also represented (see Table 2 for station names). LIML routine soundings are reported as magenta lines. The variation range of the surrounding crest height is also indicated.

ACPD
13, 19121–19171, 2013

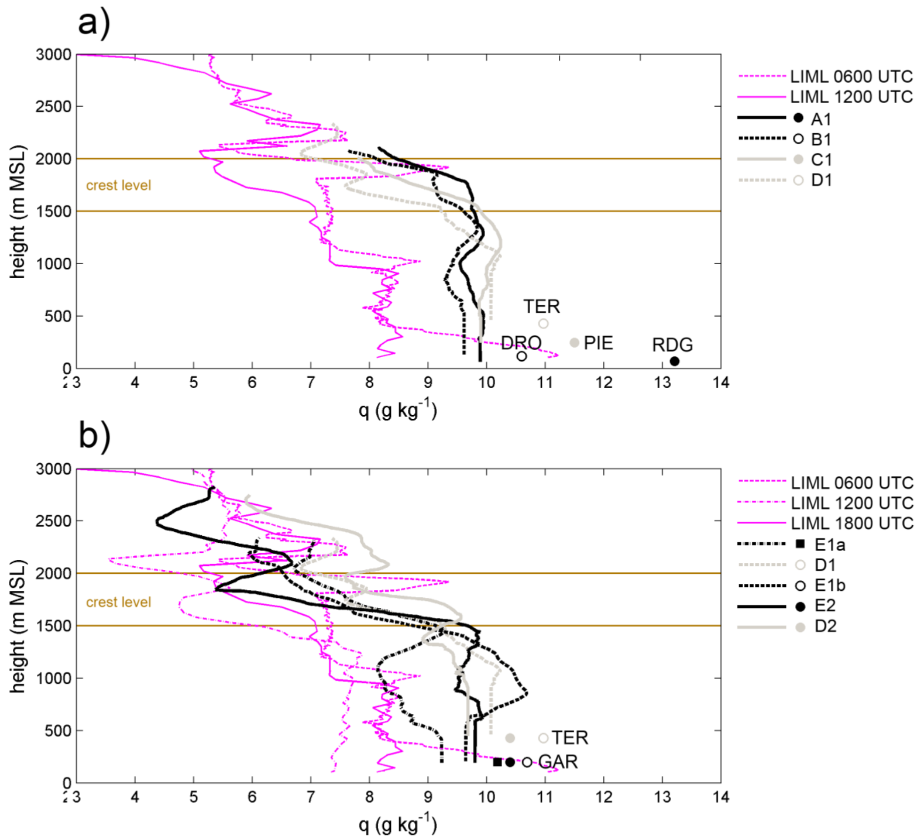

Fig. 7. As in Fig. 6 but for water vapour mixing ratio.

ACPD
13, 19121–19171, 2013

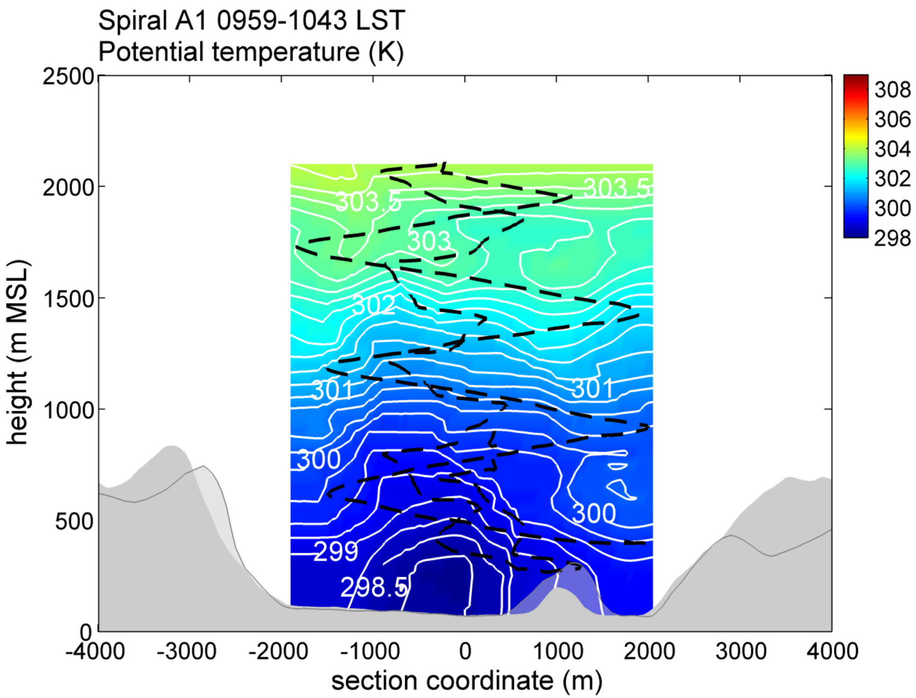

Fig. 8. Cross-valley vertical section of RK-interpolated potential temperature field for spiral A1 (in colour); contour interval is 0.25 K (in white). The correspondent valley topography is indicated by grey shading. The cross section is taken immediately down-stream of Mt. Brione relief (semi-transparent grey shading), i.e. ∼ 3 km inland from Lake Garda's shoreline. Accordingly, the horizontal coordinate marks the cross-valley direction (WNW–ESE). The black dashed line represents the projection of the motorglider's trajectory over the considered section.

ACPD
13, 19121–19171, 2013

Analysis of the *Ora del Garda* wind from airborne measurements

L. Laiti et al.

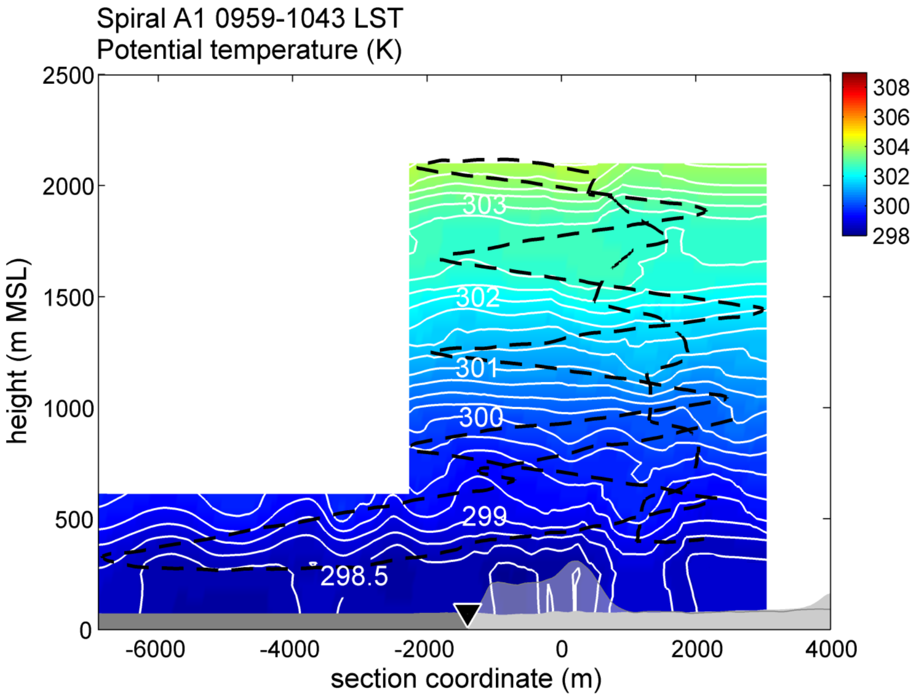

Fig. 9. As in Fig. 8, but for a longitudinal (along-valley) vertical section. Dark grey shading corresponds to Lake Garda and the black triangle indicates the shoreline. The section is taken immediately W of Mt. Brione (semi-transparent grey shading), i.e. in the middle of the lower Sarca Valley. Accordingly, the horizontal coordinate marks the along-valley direction (SSW–NNE).

ACPD
13, 19121–19171, 2013

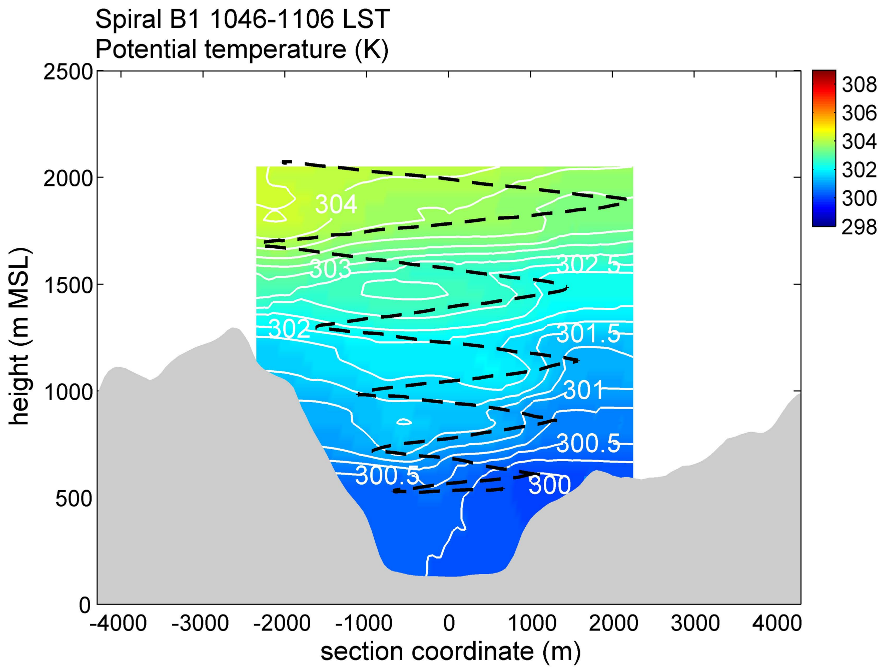

Fig. 10. As in Fig. 8, but for spiral B1. The horizontal coordinate marks the cross-valley direction (WSW–ENE).

ACPD
13, 19121–19171, 2013

Analysis of the *Ora del Garda* wind from airborne measurements

L. Laiti et al.

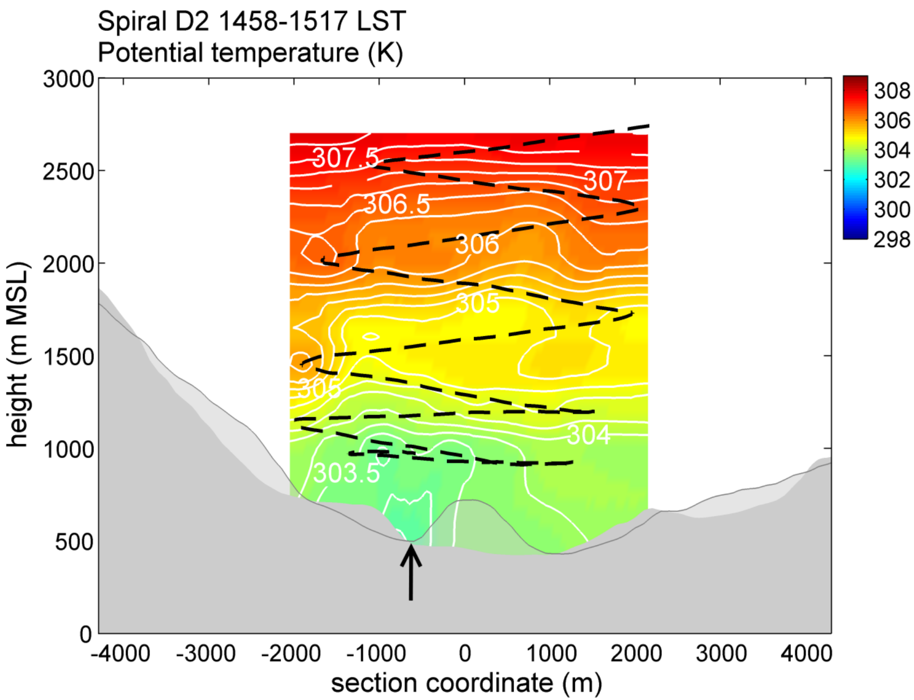

Fig. 11. As in Fig. 8, but for spiral D2. The horizontal coordinate marks the local cross-valley direction for the Lakes Valley (NNW–SSE). The cross section is taken ∼ 1 km up-stream of the Terlago saddle ridge, whose lowest point's projected position is indicated by the black arrow. A profile of the topography immediately up-stream of the selected section is also shown (semi-transparent grey shading).

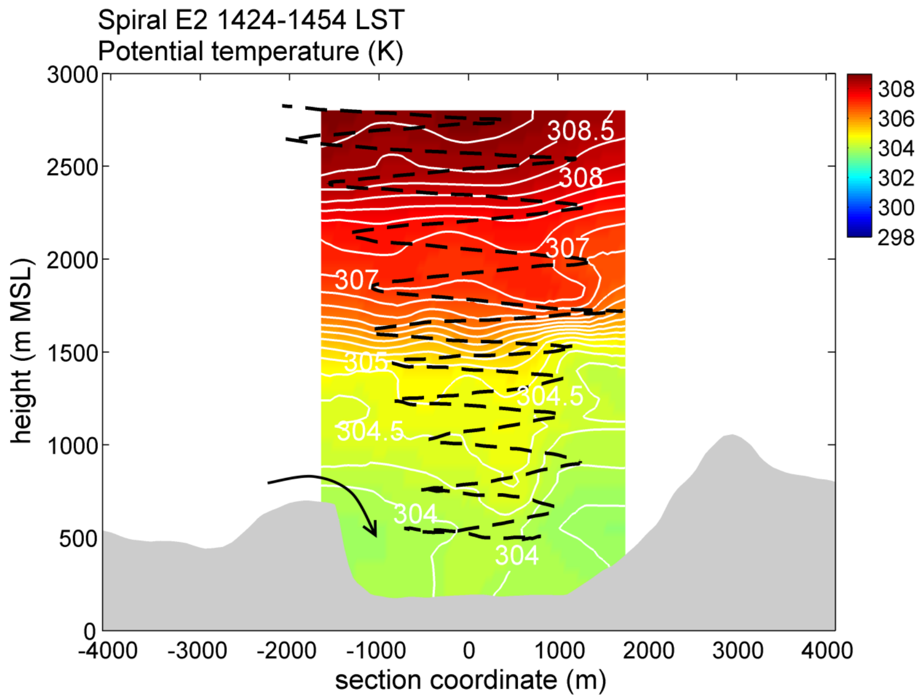

Fig. 12. As in Fig. 8, but for spiral E2. The horizontal coordinate marks the cross-valley direction for the Adige Valley (W–E). The black arrow on the left indicates the *Ora del Garda* overflowing direction from the Lakes Valley through the Terlago saddle.